Electrochemical Energy Reviews (2018) 1:84–112
https://doi.org/10.1007/s41918-018-0003-2

REVIEW ARTICLE

Carbon-Based Metal-Free Electrocatalysis for Energy Conversion, Energy Storage, and Environmental Protection

Chuangang Hu[1] · Ying Xiao[1,2] · Yuqin Zou[2] · Liming Dai[1,2,3]

Received: 24 November 2017 / Revised: 9 January 2018 / Accepted: 8 February 2018 / Published online: 17 March 2018

Abstract

Carbon-based metal-free catalysts possess desirable properties such as high earth abundance, low cost, high electrical conductivity, structural tunability, good selectivity, strong stability in acidic/alkaline conditions, and environmental friendliness. Because of these properties, these catalysts have recently received increasing attention in energy and environmental applications. Subsequently, various carbon-based electrocatalysts have been developed to replace noble metal catalysts for low-cost renewable generation and storage of clean energy and environmental protection through metal-free electrocatalysis. This article provides an up-to-date review of this rapidly developing field by critically assessing recent advances in the mechanistic understanding, structure design, and material/device fabrication of metal-free carbon-based electrocatalysts for clean energy conversion/storage and environmental protection, along with discussions on current challenges and perspectives.

Graphical Abstract

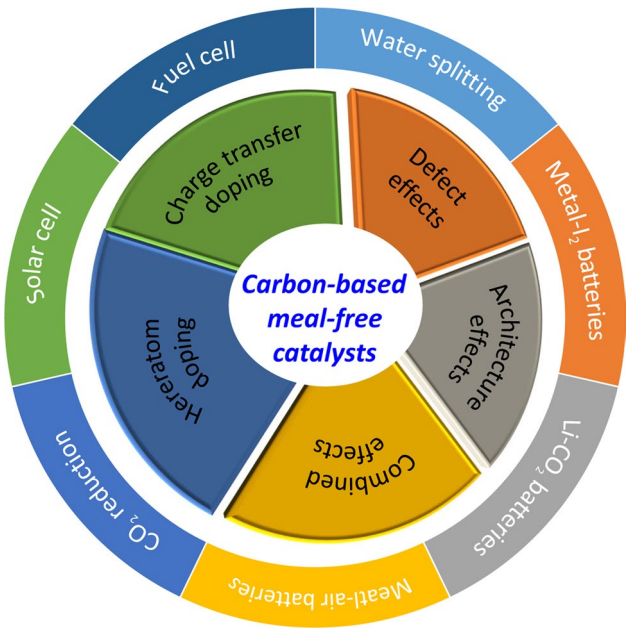

Keywords Metal-free electrocatalysis · Carbon-based catalysts · Energy conversion and storage · Environmental protection

The original version of this article was revised: The title of the article was incorrect.

Extended author information available on the last page of the article

PACS 81.05.U-

1 Introduction

Because of accelerating global energy consumption and growing environmental concerns, the need to develop clean and sustainable energy conversion and storage systems, such as fuel cells, dye-sensitized solar cells, metal-air batteries, and Li-CO_2 batteries, is of great importance [1–3]. These renewable energy technologies rely on several important reactions, including oxygen reduction reaction (ORR), oxygen evolution reaction (OER), hydrogen evolution reaction (HER), and CO_2 reduction reaction (CO_2RR), all of which require catalysts. Currently, metal-based catalysts are widely used but suffering from multiple competitive disadvantages, such as low selectivity, poor durability, and negative environmental impacts [4]. Therefore, the development of earth-abundant, cost-effective, stable, and catalytically active metal-free alternatives is highly desirable for application in renewable energy technologies.

The recent availability of carbon nanomaterials, such as graphene, carbon nanotubes (CNTs), graphite nanoplatelets, and three-dimensional (3D) carbon architectures offer new opportunities for the development of advanced metal-free catalysts [4]. Because of high abundance, high electrical conductivity, structure tunability at the atomic level, high selectivity, strong tolerance to acidic/alkaline conditions, and eco-friendliness [4, 5], many nanostructured carbon materials have been developed as metal-free catalysts with impressive electrocatalytic performances for ORR, HER, OER, and/or CO_2RR, key reactions involved in energy conversion/storage and environmental protection processes [3, 6–9]. The electrocatalytic performances of metal-free carbon-based catalysts were further found to be tuneable through the regulation of the nanoparticles size, macrostructures, and electrode architectures, along with the introduction of heteroatoms (doping) and defects [8, 9].

In this review, general strategies for creating active sites on carbon-based catalysts for various electrochemical reactions will first be discussed. Because ORR, OER, and HER have been reviewed in several previously published articles [4, 10–12], the focus in this review will be on recent advances and new reactions (e.g., CO_2RR, multifunctional electrocatalysis). A critical overview of efficient methods for developing carbon-based metal-free catalysts for various energy conversion/storage and environmental protection devices, including ORR in fuel cells [13–17], ORR and OER in metal-air batteries [18–28], OER and HER in water-splitting units [29–31], I^-/I^{3-} reduction in dye-sensitized solar cells [32–35], and CO_2RR in Li-CO_2 batteries [36–42] will then be provided. Finally, perspectives and challenges in this fast-growing and significant field are outlined.

2 Graphitic Carbon Materials

Carbon exists in three forms (i.e., amorphous carbon, graphite, and diamond) each with different carbon atom arrangements and properties [43, 44]. For example, graphite is a soft, black, and stable common form of carbon with strong covalent bonding in the carbon plane and much weaker van der Waals interactions in the transverse direction between layers. Diamond is hard and transparent, with each carbon atom bonding to four other carbon atoms in a regular repetitive pattern.

2.1 Carbon Nanotubes

A carbon nanotube (CNT) can be seen as a graphite sheet rolled into a nanoscale tubular to form a single-wall carbon nanotube (SWCNT) or as concentric graphene tubes attached around the core of a SWCNT to form a multi-walled carbon nanotube (MWCNT). Nanotubes usually possess diameters ranging from a few angstroms to tens of nanometres and lengths of up to several centimeters and even submeters [45, 46]. The peculiar hollow geometry, coupled with a conjugated all-carbon structure, allows CNTs to exhibit many intriguing electrical, mechanical, and thermal properties that are absent from other members of the carbon family. In particular, CNTs can exhibit semiconducting or metallic behaviors depending on the diameter and helicity of the arrangement of graphitic rings in the walls [47]. High surface area is another important property of CNTs, with theoretical surface areas of SWCNTs reaching 1315 $m^2\ g^{-1}$ [48]. Because of the unique structures and extraordinary electrical, mechanical, and optical properties, CNTs are promising for various applications [49–51], ranging from composite materials to electronic and energy-related devices [52–58].

2.2 Graphene

Graphene, a one-atom-thick planar sheet of sp^2-bonded carbon in a honeycomb network, is a rising star in materials sciences, physics, and chemistry since its discovery in 2004 [59]. Like CNTs, graphene possesses many excellent properties, including large specific surface area (2630 $m^2\ g^{-1}$) [60], outstanding thermal conductivity (ca. 5000 $W\ m^{-1}\ K^{-1}$ for single-layer graphene) [61], high Young's modulus (1.0 TPa) [62], good electrical conductivity (106 $S\ cm^{-1}$),

and excellent charge mobility (200,000 $cm^2\ V^{-1}\ s^{-1}$) [63]. Moreover, single-layer graphene is very transparent and therefore can be used as a transparent electrode [60]. Superior to CNTs in many physical and chemical properties, graphene has attracted a great deal of interest in a host of potential applications, including fuel cells, solar cells, batteries, supercapacitors, field-effect transistors (FETs), sensors, and actuators [58–60, 64–66].

2.3 Nanostructured Graphite and Nanodiamond

Nanostructured graphite with specific surface areas over 400 $m^2\ g^{-1}$ is produced by mechanical milling in a hydrogen atmosphere [67] in which a large amount of hydrogen can be incorporated into fragmented nanostructured graphite matrixes during the milling process [68]. The hydrogen content, size, and structure of nanostructured graphite can be controlled by regulating milling conditions (e.g., time) [67]. Apart from mechanical milling, hot-filament CVD has also been used for the production of nanostructured graphite [69].

Nanodiamonds (NDs) possess diamond structures on the nanometre scale and exhibit unique optoelectronic, mechanical, thermal, and biological properties useful in a variety of important applications [70–74]. Single crystals of cubic diamond nanoparticles of 4–5 nm in size were first discovered in 1963 by a group of Soviet scientists detonating an oxygen deficient 2,4,6-trinitrotoluene/hexogen composition in an inert media [75]. Subsequent reports on the use of a stirred-media milling technique to well-dispersed ND particles [76, 77] have led to the preparation of novel dispersed ultra-nanocrystalline diamonds (4–5 nm). In addition to unique mechanical properties and environmental stability, nanodiamonds possess a high dielectric constant (3.5 K), a high electrical breakdown strength (787 V/μ), high operating temperatures (> 250 °C), and a low dissipation factor of 0.05% (at 25 °C, 1 kHz), making nanodiamonds promising candidate materials for important applications, such as microelectromechanical systems (MEMS) [78], field emission displays [70], electrochemical analyses [79], nanomedicines [72], and energy storage systems [74].

More recently, hierarchically structured 3D carbon nanomaterials (e.g., 3D pillared CNT-graphene architecture [80, 81]) have attracted considerable attention. Possessing a conjugated all-carbon structure with unusual molecular symmetries and hierarchal architectures, CNTs, graphene, and their 3D hybrids show interesting electronic, photonic, magnetic, electrocatalytic, and mechanical properties that are attractive for a wide range of potential applications. Of particular interest, hierarchically structured carbon nanomaterials have been studied as catalysts for a wide range of energy-related and environmental protection applications [82–84].

3 Design Strategies of Graphitic Carbon Catalysts

3.1 Heteroatom-Doping

Since the discovery of the first low-cost, but efficient, platinum alternative carbon-based metal-free catalysts (i.e., nitrogen-doped vertically aligned carbon nanotube array, VA-NCNTs) for ORR in 2009 in alkaline electrolyte [85], various carbon-based catalysts doped with a variety of different heteroatoms (N, B, S, P, F, etc.) have been reported [10]. These heteroatom dopants, either electron-rich (e.g., N) or electron-deficient (e.g., B), play at least two critical roles in activating graphitic sp^2 carbon for ORR: (1) breaking the electroneutrality (χ) and/or spin distribution symmetry of sp^2 carbon atoms within the graphitic network to create charge/spin redistribution to facilitate the chemisorption of O_2 and/or ORR intermediate products, and (2) effectively utilizing heteroatom-doping-induced electron transfer for O_2 reduction. Density functional theory (DFT) simulations indicate that the electrocatalytic activity of carbon-based catalysts is related to the electron spin and atomic charge density redistribution caused by doping [86, 87].

So far, the introduction of N atoms into graphitic carbon has been found to be the most effective heteroatom dopant to improve catalytic performances as N atoms possess similar atomic sizes as carbon and can efficiently donate a lone pair of electrons to the π-conjugation system of sp^2 carbon networks [4, 85]. Doped N atoms can change the chemisorption mode of O_2 from the usual end-on adsorption (Pauling model) at the N-free CNT surface to a side-on adsorption (Yeager model) at the N-doped carbon electrode (Fig. 1a, b). Because of this, N-doping induces charge transfer, and together with parallel diatomic O_2 adsorption, can effectively lower the ORR potential and weaken O–O bonds to facilitate oxygen reduction at the N-doped carbon electrode [85]. Similar to N ($\chi = 2.50$) atoms, B ($\chi = 2.04$) and F ($\chi = 3.98$) atoms also present large electronegativity differences from C ($\chi = 2.55$), creating charged sites for ORR after being doped into sp^2 carbon lattices either on the carbon basal plane or at the edge sites. Unlike N dopants however, B atoms can also act as positively charged sites for ORR because B atoms possess lower electronegativity than C (Fig. 1c) [88]. Similarly, the high electronegativity of F atoms can induce adjacent C polarization to create active sites. In addition, S ($\chi = 2.58$), possessing similar electronegativity to C and expected to have low effects on charge distribution and thus low ORR activity, [89] actually facilitates high ORR performance because the spin density in S-doped carbon is slightly higher than that in pure carbon. Instead of the

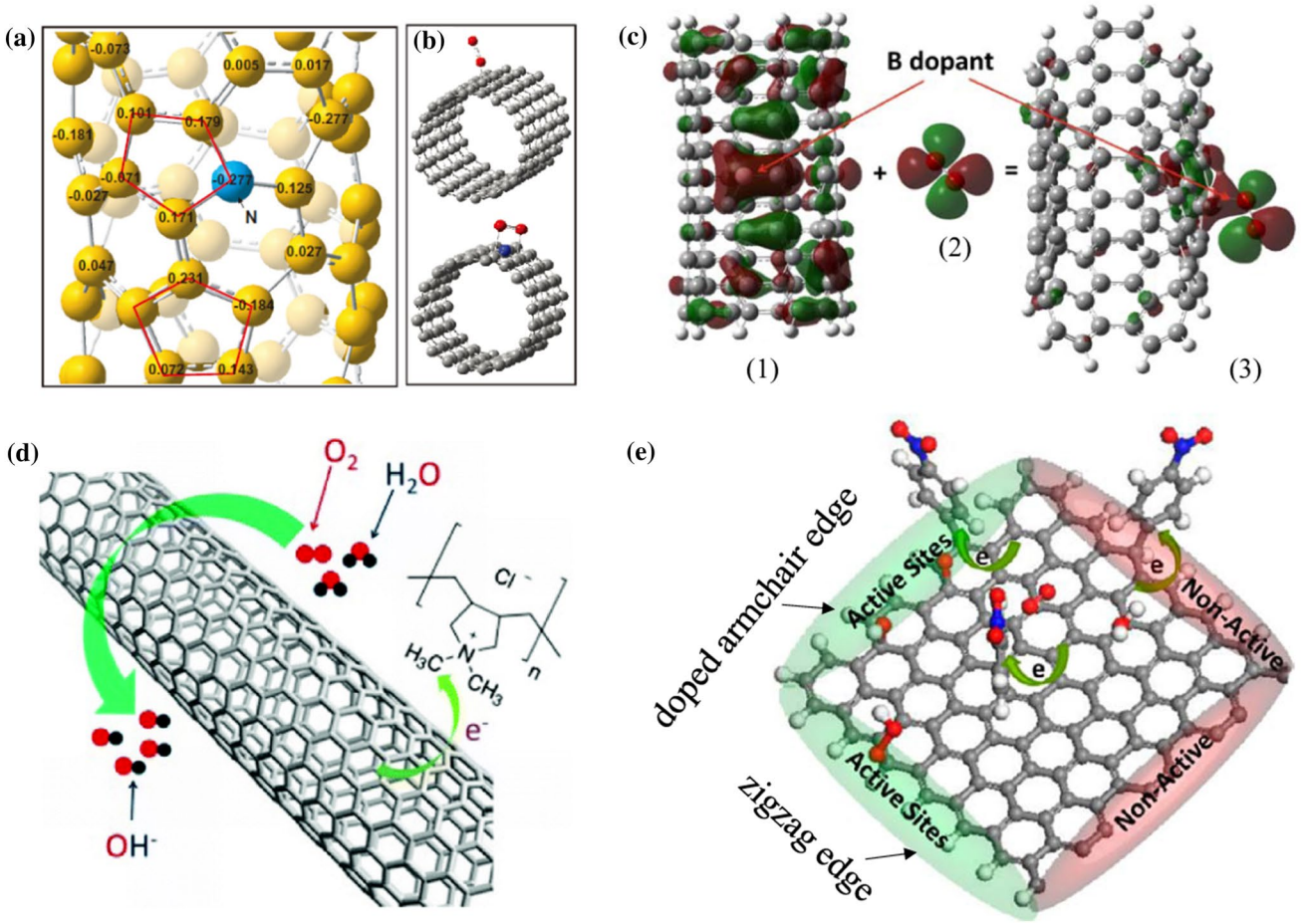

Fig. 1 **a** Calculated charge density distribution for NCNTs. **b** Schematic representations of possible adsorption modes of an oxygen molecule in CCNTs (top) and NCNTs (bottom). Reproduced with permission from Ref. [85], Copyright 2009, AAAS. **c** Important molecular orbitals involved in O_2 adsorption on BCNT (5, 5). (1) Spin-down HOMO-1 of BCNT (5, 5). (2) LUMO of triplet O_2. (3) Spin-down HOMO-2 of O_2-BCNT (5, 5). Reproduced with permission from Ref. [88], Copyright 2011, Wiley–VCH.) **d** Illustration of charge transfer process and oxygen reduction reaction on PDDA-CNT. Reproduced with permission from Ref. [107], Copyright 2011, American Chemical Society. **e** A model of nitrobenzene molecular-doped graphene for ORR based on first-principles calculations. The zigzag edge, doped armchair edge, and opposite-side edge of the doped nanoribbon. Reproduced with permission from Ref. [109], Copyright 2016, American Chemical Society

substitution of sp^2 carbon atoms, S in carbon lattices is often in the form of a thiophene-like structure because of its larger atomic radius relative to C. Covalently bonded S, especially sulfur oxide, at zigzag or armchair edges of carbon planes can also create polarized zones that serve as active sites for ORR. In general, a large number of chemical species in the form of either substitution or attachment to sp^2 carbon can induce asymmetric spin density and/or atom charge density to promote ORR electrocatalysis [89].

There are multiple factors, including the electronic structure of heteroatoms, the content and distribution of dopants, and the conductivity and architecture of resulting materials, that can affect the optimized performance of heteroatom-doped carbon catalysts. Thus, an increase in the heteroatom-doping content may not always enhance carbon-based catalyst performance [13]. In fact, the type of heteroatom dopant is of vital importance in the performance enhancement for metal-free carbon catalysts. In particular, nitrogen can exist in many different forms in N-doped carbon catalysts, such as pyridine-like, pyrrole-like, graphitic nitrogen, and pyridine-N-oxide [3, 90]. Therefore, the understanding of the effects of N-dopant chemical nature on electrocatalytic performance is of great importance. For example, by using highly oriented pyrolytic graphite (HOPG) model catalysts with well-defined π conjugation and well-controlled dopant N species, pyridinic N was found to be the active site for ORR in acidic electrolytes [91]. Another independent study demonstrated that pyridine-N-oxide did not possess any ORR activity in which the complete loss of

pyridine-N-oxide groups after long-term stability tests had no effect on catalyst activity [92].

Recently, Yang et al. demonstrated that electron-donating quaternary N sites were responsible for ORR, whereas electron-withdrawing pyridinic N moieties served as active sites for OER in alkaline electrolytes [93]. Clearly, further combined theoretical and experimental research is needed to better understand the effects of the chemical nature of dopants.

Even with the same doping elements and types, heteroatom-doped carbon catalyst performances vary with dopant locations. For example, doping heteroatoms at the edge of graphene sheets with minimal damage to the carbon basal plane can impart solubility and electrocatalytic activity and largely retain the physicochemical properties of the pristine graphene [94, 95]. Because the dangling bonds at the edge of graphene sheets have been demonstrated to be more reactive than covalently bonded carbon atoms within the basal plane [96], edge-doped/functionalized carbon/graphene can act as active metal-free catalysts for many specific applications [94]. Heteroatoms, such as Cl, Br, I, S, Se, and Sb, have also been introduced at the edge of graphene nanoplatelets (x-GnPs) through the ball milling of graphite powder in the presence of appropriate chemicals, such as Cl_2, Br_2, I_2, S_8, Se, and Sb [89, 97–103].

The performance of heteroatom-doped carbon catalysts can be further improved through co-doping with different heteroatoms (e.g., N and B, N and S, N and P). This is because increased numbers of dopant heteroatoms and electronic interactions between different doped heteroatoms often generate additional synergistic effects than single heteroatom-doped counterparts [104]. With N as the primary dopant, B, S, and P can be used as secondary elements for co-doping carbon [4, 105]. Here, it was found that S-doping, followed by P-doping, greatly promotes HER. The doping of graphene with elements such as N, S, and F was also found to create active sites for ORR in both acidic and alkaline media [17].

3.2 Intermolecular Charge Transfer

In addition to the heteroatom-doping-induced intramolecular charge transfer or spin redistribution that boosts electrocatalytic activities of carbon-based catalysts described above, charge-transfer doping graphitic all-carbon carbon nanomaterials with electron acceptor(s) or donor(s) can induce intermolecular charge transfer to impart catalytic activities to heteroatom-free carbon catalysts [106–108]. Much like heteroatom-doping-induced intramolecular charge redistribution to facilitate ORR processes, the physical adsorption of certain (macro)molecules onto all-carbon CNTs [107] or graphene sheets [108] can cause intermolecular charge transfers to induce ORR electrocatalytic activities similar to those of commercial Pt/C catalysts. The first experimental evidence for intermolecular-charge-transfer-induced ORR catalytic activities of carbon-based catalysts was observed as early as 2011 by Wang et al. [107]. In their particular case, quaternary ammonium functional groups along physically adsorbed PDDA backbones possessed a strong electron-accepting ability to withdraw electrons from carbon atoms in nanotube carbon planes to induce net positive charge (Fig. 1d), facilitating the ORR catalytic activities of dopant-free CNT/graphene adsorbed with PDDA chains [107, 108]. Subsequently, graphene molecularly doped with nitrobenzene for ORR was investigated using first-principles calculations [109]. In this investigation, the active centers were found to be zigzag edges, doped armchair edges, and opposite-side edges of doped zigzag nanoribbons with high asymmetry spin/charge densities induced by intermolecular charge transfer (Fig. 1e).

The demonstration that all-carbon CNTs/graphene sheets can be converted into efficient metal-free ORR electrocatalysts simply through adsorption-induced intermolecular charge transfer presents considerable avenues for the cost-effective preparation of various metal-free catalysts for ORR and even new catalytic materials for applications beyond ORR. Therefore, the aforementioned strategies should provide general approaches to the design of metal-free carbon-based catalysts for a wide range of applications.

3.3 Defect-Induced Charge Transfer

Like all crystalline materials, certain amounts of disorders or defects are unavoidable in graphitic carbons because of the second law of thermodynamics [110]. In general, intrinsic defects in nanocarbon structures, including vacancies, voids, Stone–Wales defects, dislocation, and grain boundaries [110–112], often result from the absence of certain atoms and/or reconstruction of the lattice, leading to breaks in electron–hole symmetry [113]. These defective regions in graphitic carbon materials, with dangling groups, hydrogen saturation, or reconstruction free from dangling groups, have been widely demonstrated to alter local densities of π-electrons and increase chemical reactivities [114]. In-plane topological defects (e.g., pentagons and heptagons, instead of hexagonal rings) usually exist in graphitic carbon skeletons. These defects can also locally induce Gaussian curvatures to alter bond lengths and rehybridize electron orbitals [114], leading to electron redistribution and therefore high ORR activities [115]. In addition, the ORR performance of N-doped graphene can also be greatly enhanced by Stone–Wales defects, which decrease the HOMO–LUMO energy gap of nanoscale graphene domains and change reaction pathways [116, 117].

Line defects (e.g., edges, cracks, voids [113]) in graphene sheets were revealed to be also efficient for electrochemical

catalysis (e.g., ORR) [116]. On the edge side, localized states are induced along the edge length to modify local band structures and change the electron properties of the nanocarbon. Pentagon rings at the zigzag edge (or pentagon–pentagon–octagon chain) were also found to significantly modify graphene edges and induce local charge/spin polarization for catalyzing ORR (Fig. 2a) [118].

Well-defined pore distributions and defects can affect the catalytic activity of carbon-based catalysts [111, 112, 119–122]. In 2015, Jin et al. reported a new class of ORR catalysts based on graphene quantum dots supported by graphene nanoribbons with ORR performances comparable to or even better than that of Pt/C electrodes [119]. These performances were attributed to the presence of numerous edge defects on quantum dots and

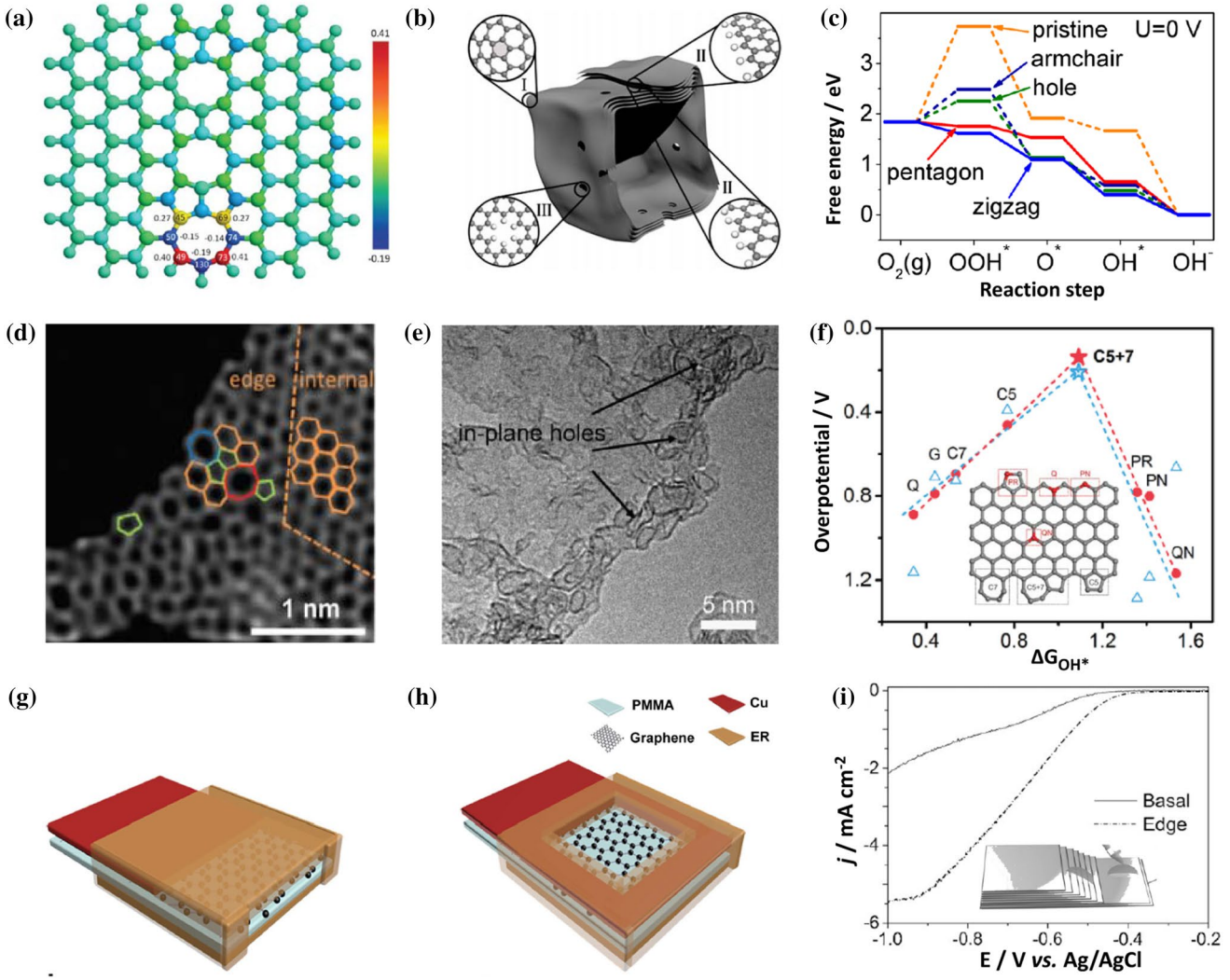

Fig. 2 **a** Spin density distribution on the graphene cluster containing a line defect with an odd number of octagon and fused pentagon carbon rings. Reproduced with permission from Ref. [118], Copyright 2015, Royal Society of Chemistry. **b** Schematic structural characteristics of carbon nanocages. I, II, and III represent three typical defective locations, i.e., the corner (pentagon defect), the broken fringe (Zigzag edge and Armchair edge), and the hole, respectively. **c** Free energy diagrams from DFT calculations for ORR activities of different defects. Reproduced with permission from Ref. [120], Copyright 2015, American Chemical Society. **d** High-angle annular dark-field scanning transmission electron microscopy (HAADF-STEM) image of DG with an acceleration voltage of 80 kV. Hexagons, pentagons, heptagons, and octagons are labeled in orange, green, blue, and red, respectively. Reprinted with permission from Ref. [121], Copyright 2016, Wiley–VCH. **e** High-resolution transmission electron microscopy (HR-TEM) image of NGM. **f** The proposed volcano plots of overpotential versus adsorption energy of OH*. The inset schematically represents graphene nanoribbon with different types of N-doping or topological defects used for DFT calculations. Reproduced with permission from Ref. [111], Copyright 2016, Wiley–VCH. Schematic illustration of the edge-based (**g**) and basal plane-based (**h**) electrodes. Reproduced with permission from Ref. [125], Copyright 2016, Royal Society of Chemistry. **i** LSV curves of a ORR test in a 1.0 M KOH droplet located on the edge or basal plane of HOPG. The inset illustrates the micro-apparatus for the ORR tests. Reproduced with permission from Ref. [96], Copyright 2014, Wiley–VCH

graphene nanoribbons, coupled with efficient charge transfer between the two. Jiang et al. also developed defective carbon nanocages with ORR activities better than that of B-doped carbon nanotubes and comparable to that of N-doped carbon nanostructures (Fig. 2b) [120] with DFT calculations indicating that pentagon and zigzag edge defects were responsible for the observed high ORR activity for the defective carbon nanocages (Fig. 2c) [120]. Recently, defective graphene (DG) materials have also been prepared from N-doped precursors using a facile nitrogen removal procedure (Fig. 2d) [121] which can create different types of defects for multifunctional catalytic reactions such as ORR, OER, and HER. In a similar study, a defective porous carbon (PC) material with only carbon and oxygen was synthesized through the carbonization of Zn-MOF (IRMOF-8) at 950 °C, followed by the removal of Zn atoms during the calcination process and exhibited excellent electrocatalytic activity, molecular selectivity, and long-term durability [122]. More recently, metal-free carbon-based ORR/OER catalysts with topological defects were fabricated through the direct carbonization of carbon/nitrogen precursors on MgO templates [111]. These as-obtained defective rich graphene materials consisting of predominantly few-layer thick graphitic carbon sheets with abundant in-plane nanopores (Fig. 2e) exhibited more favorable ORR performances than Pt/C with similar onset potentials, higher current densities, and much better durabilities in O_2-saturated 0.10 M KOH. Here, DFT calculations (Fig. 2f) revealed that topological defects at the edge play an even more important role than doping and edge effects on catalytic performance with the N-free intrinsic defect of an adjacent pentagon and heptagon being identified as the optimal defect configuration to induce catalytic activities for both ORR and OER, as evidenced by the peak position in volcano plots (Fig. 2f). Additionally, dangling bonds located at the edge of sp^2 nanocarbons after saturation by hydrogen can act as high-energy sites and catalytic centers for many acid–base or redox reactions [123]. It was demonstrated that graphene edges showed a two-time higher ORR reactivity, a 4 orders of magnitude larger specific capacitance, and a faster electron-transfer rate than basal planes (Fig. 2g, h) [124, 125]. The observed edge enhanced electrocatalytic activity was further confirmed by precise measurements of ORR activity at the edge or basal-plane regions of HOPG using a micro-apparatus (Fig. 2i) [96]. In addition, edge-rich and dopant-free CNTs and graphene were developed as highly efficient ORR electrocatalysts [126], and the activity origin of aerobic oxidation in porous graphene oxide (GO) catalysts was elucidated to be caused by edge sites with unpaired electrons and carboxylic groups favorable for O_2 trapping and electron transport. Recent developments in defective carbon catalysts have demonstrated the critical role of edge and intrinsic defects in regulating catalytic performance of carbon catalysts [94, 119], and this is an area that will clearly benefit from further research.

3.4 Combined Effects

The incorporation of heteroatom(s) into graphitic carbon frameworks can effectively modulate the electronic structures of surrounding carbon atoms and tune local charge density distributions to generate catalytic activity, as described above. Although this incorporation is significantly affected by dopant types, dopant locations, and dopant contents, many other factors also affect the electrochemical catalytic performance of carbon catalysts doped with or without heteroatoms. In this context, Dai's group was the first to report significantly enhanced ORR activities for N,B-co-doped CNTs compared with single N- or B-doped CNTs [127]. To demonstrate the synergistic effects induced by co-doping, Hu's group intentionally controlled the locations of co-dopant elements to prepare two types of N,B-co-doped CNTs dominated by bonded or separated B and N, both of which exhibited distinct ORR performances (Fig. 3a) [128]. Their experimental and theoretical results indicated that the separated B and N can turn inert CNTs into ORR electrocatalysts whereas the bonded B and N cannot. Similar phenomenon was independently observed by Qiao's group [129]. As far as published results on co-doping or even multiple doping [8, 26, 29, 104, 130] are concerned, although much progress has been made, more is needed.

For heterogeneous catalysis, the active sites of a catalyst need to be exposed at the surface rather than at the bulk structure to maximize accessibility to reactants so as to increase the catalytic efficiency. Therefore, it is important to develop catalysts with desired macrostructures to achieve high exposures of active sites. For this purpose, N-doped carbon coaxial nanocables, consisting of a pristine CNT core and an N-doped carbon layered shell, were demonstrated to be an ideal metal-free carbon-based catalyst for both ORR and OER (Fig. 3b) [130]. In this case, the intact inner tubes can act as effective electronic conducting pathways for effective charge transfer through electron tunneling between the outer wall and inner tubes and the outer wall can provide reaction sites for the absorption and dissociation of OH^- and OOH* species. Similarly, N- and S-doped CNTs with superb bifunctional catalytic activities for both HER and OER in alkaline solution were also developed by improving active-site exposure (Fig. 3c) [131]. These studies confirm that observed excellent bifunctional catalytic performances are attributable to co-doping, coupled with the efficient mass and charge transfer of carbon catalysts with high active site exposure. High HER performance has also been achieved by coupling graphitic carbon nitride (g-C_3N_4) with N-doped graphene (N-G) to combine intermolecular charge transfer

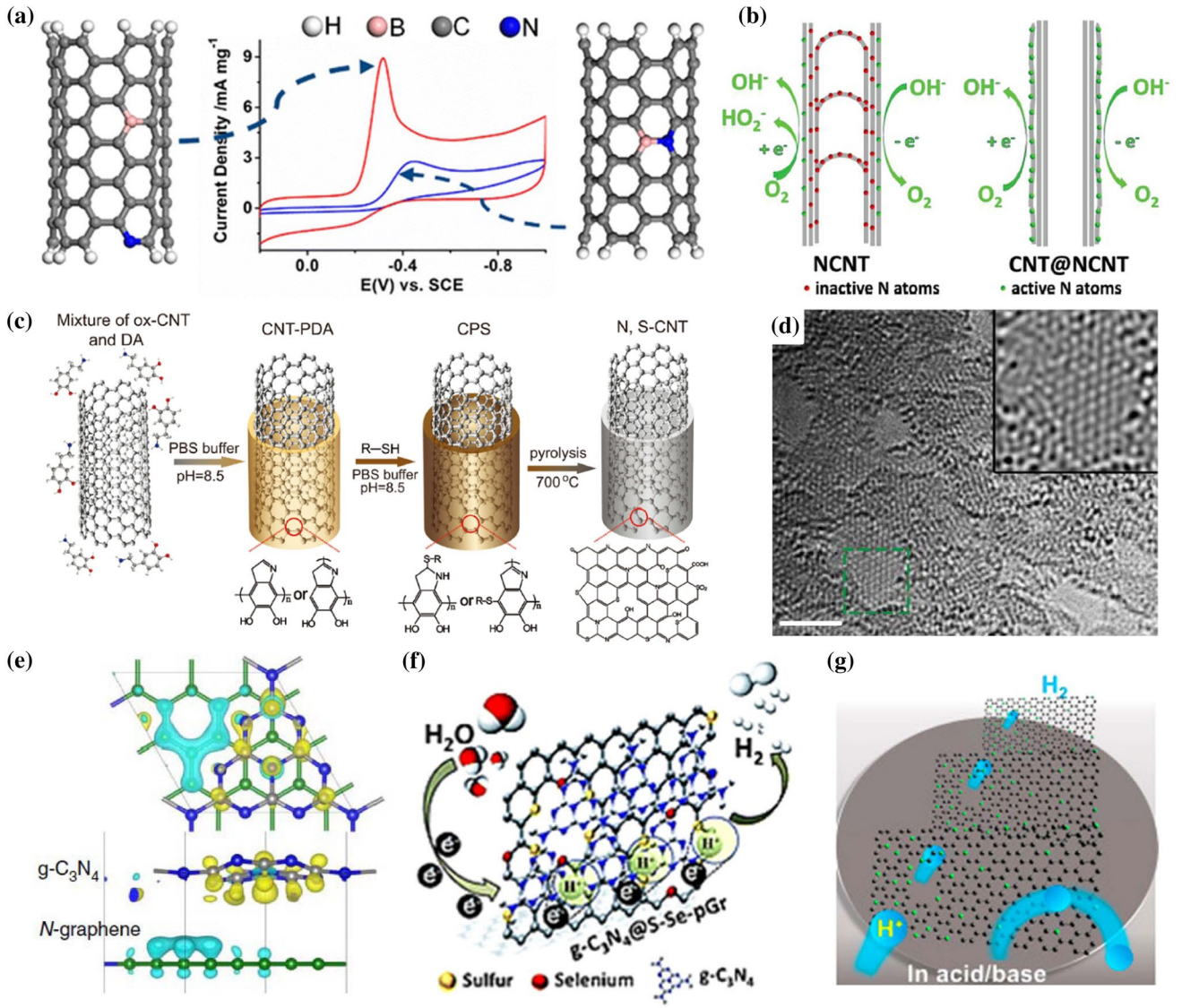

Fig. 3 **a** Schematic diagrams of two types of B,N-co-doped CNTs and corresponding ORR activities. Separated B,N-co-doped CNTs present high ORR activity, whereas bonded B,N-co-doped CNTs present low ORR activity. Reprinted with permission from Ref. [128], Copyright 2013 American Chemical Society. **b** NCNTs with bulk doping of N atoms, as well as CNT@NCNT coaxial nanocables with surface N-enriched nitrogen doping. Reprinted with permission from Ref. [130], Copyright 2014 Wiley–VCH. **c** Fabrication of N, S-CNT following a two-step "graft-and-pyrolysis" route. Oxidized CNT (ox-CNT) was mixed with dopamine (DA) in PBS buffer to obtain CNT-PDA hybrid. The addition of R-SH (2-mercaptoethanol) into CNT-PDA followed by pyrolysis led to N, S-CNT. Reprinted with permission from Ref. [131], Copyright 2011 Wiley–VCH. **d** Interfacial electron transfer in C_3N_4@NG. Yellow and cyan iso-surfaces represent electron accumulation and electron depletion; the iso-surface value is 0.005 e $Å^{-3}$. Reprinted with permission from Ref. [132], Copyright 2015 Nature Publishing Group. **f** Scheme of the HER on g-C_3N_4@S-Se-pGr. Reprinted with permission from Ref. [133], Copyright 2015 Wiley–VCH. **g** Schematic diagram of HER on Nr-HGM. Reprinted with permission from Ref. [137], Copyright 2015 Elsevier B.V

with heteroatom-doping [132]. DFT calculations indicate an apparent electron transfer from conductive N-G to g-C_3N_4, leading to an electron-rich region on the g-C_3N_4 layer and a hole-rich region on the N-graphene layer (Fig. 3d, e). In a similar but independent study, g-C_3N_4 was coupled with S,Se-co-doped porous graphene (pGr) through a scalable approach to prepare a catalyst (Fig. 3f) [133] that produced high HER performance and robust stability over a wide pH range. These studies demonstrate the effectiveness of chemical and electronic coupling to promote proton adsorption and reduction kinetics.

In typical gas-involved heterogeneous catalysis, porous structures with massive pore edges can promote interfacial catalytic reactions and subsequent gas desorption [134,

135]. Therefore, the porosity of carbon-based catalysts is another critical factor in controlling catalytic activities, and the construction of carbon catalysts with highly porous or hybrid macrostructure of large surface areas is highly desirable. Because of this, the catalytic performance of crumpled graphene sheets can be significantly enhanced by generating nanoholes within the constituent graphene layers. In this context, N-doped graphene materials with relatively uniform mesopores (MPG) have been synthesized using a micelle-template, followed by N-doping, as effective HER catalysts [136]. N-rich holey graphene monoliths (Nr-HGM) have also been prepared by pyrolysis of GO and ammonium sulfate [137] to opening "windows" for efficient mass transfer of electrolytes and/or hydrogen, and thus improved HER activity (Fig. 3g). Furthermore, the catalytic performance of an electrode can further be enhanced by tailoring the macrostructure of the electrode to maximize the exposure of active sites. This, coupled with controlled heteroatom-doping, creates synergistic effects [138].

4 Doped Nanocarbons as Metal-Free Electrocatalysts for Energy Devices

4.1 Carbon-Based Metal-Free ORR Electrocatalysts for Fuel Cells

Fuel cells convert chemical energy directly into electricity by electrochemically oxidizing fuels (e.g., H_2) and reducing oxygen into water, providing instant power output with high energy conversion efficiencies and high power densities without any detrimental effects on the environment [139–141]. However, noble metal catalysts (e.g., Pt) are required for hydrogen oxidation at the anode and ORR at the cathode [142, 143]. The slow ORR on the cathode is a key limiting step to the energy conversion efficiency of fuel cells and requires substantial amounts of Pt catalysts. Carbon-based ORR electrocatalysts as low-cost alternatives to Pt have attracted significant attention due to high electrocatalytic activities, long-term stabilities, high selectivities, and scalabilities of the catalysts. Excellent ORR performance, especially in alkaline media [64, 85], has been demonstrated for many carbon-based ORR catalysts.

Of particular interest, VA-NCNTs can act as metal-free electrodes to catalyze ORR processes free from CO "poisoning" with a 3-times higher electrocatalytic activity, much smaller crossover effect, and better long-term operational stability than that of commercially available platinum/C electrodes (C2-20, 20% platinumonVulcanXC-72R; E-TEK) in alkaline fuel cells. This improved catalytic performance is attributed to the electron-accepting ability of nitrogen atoms which create net positive charges on adjacent carbon atoms in the nanotube carbon plane of VA-NCNTs to enhance O_2 adsorption and attract electrons readily from the anode to facilitate ORR [85]. The elucidation of this new ORR mechanism is significant and can be applied to the development of various other metal-free catalysts for fuel cell applications and even beyond fuel cells (vide infra).

Subsequently, Rao and Ishikawa [144] prepared metal-free VA-NCNTs with a N content of 8.0 at% by template-assisted pyrolysis. The resultant VA-NCNTs exhibited an ORR activity comparable to Pt/C with a 4-electron pathway and higher ethanol tolerance than Pt/C in alkali solution. In their further evaluation in anion-exchange membrane fuel cells (AEMFCs), the VA-NCNT and Pt/C electrodes exhibited a current density of 11 and 38 mA cm^{-2}, respectively, at 0.7 V, along with a corresponding maximum power density of 37.3 and 61.7 mW cm^{-2}. Whereas the majority of recent studies on carbon nanostructured metal-free electrocatalysts focus on ORR reactions in alkaline electrolytes, fuel cells that operate with acidic electrolytes, particularly polymer electrolyte membrane fuel cells (PEMFC) [14, 15], can have a more significant economic impact. Therefore, the development of effective metal-free carbon-based catalysts for acidic electrolytes is important, though still challenging [16, 145–150].

As early as 2010, Xiong et al., investigated N-doped VA-CNT arrays as an ORR catalyst in a PEMFC analogous acidic medium and produced strong ORR signals at favorably positive potentials [151]. Compared with Pt-based catalysts, the VA-NCNT arrays resulted in a ~ 47 mV anodic shift in onset potential, and a 62% higher volumetric current density. Subsequently, Li et al. demonstrated that few-walled CNTs with the outer wall exfoliated by oxidation and high-temperature reactions with ammonia can act as an ORR electrocatalyst in both acidic and alkaline solutions [149]. N,S-co-doped CNTs (NS-CNTs) were also demonstrated to show enhanced ORR activity compared with CNTs, NCNTs, and SCNTs [150] with a much better durability than that of commercial 20 wt% Pt/C catalysts. Other examples of metal-free electrocatalysts for ORR in acidic electrolytes include N-doped SWCNTs [145], vapor-phase-polymerized PEDOT [152], pyridinic and pyrrolic N-doped graphene prepared by confined polymerization/carbonization within layered montmorillonite [90], graphene/CNT layer-by-layer composites [153], and N,F-co-doped graphite nanofibers [154]. Using pyrolysis of sulfur-doped rGO in the presence of Nafion and dimethyl formamide at 600 °C, Pham et al. [17] reported the synthesis and characterization of F,N,S-tri-doped reduced graphene oxide (F,N,S-rGO) in both acidic and alkaline PEFCs (Fig. 4a). Rotating disk electrode investigation of the F,N,S-rGO as an ORR catalyst revealed maximum power densities of 14 and 46 mW cm^{-2} for acidic and alkaline PEFCs, respectively (Fig. 4b) [17].

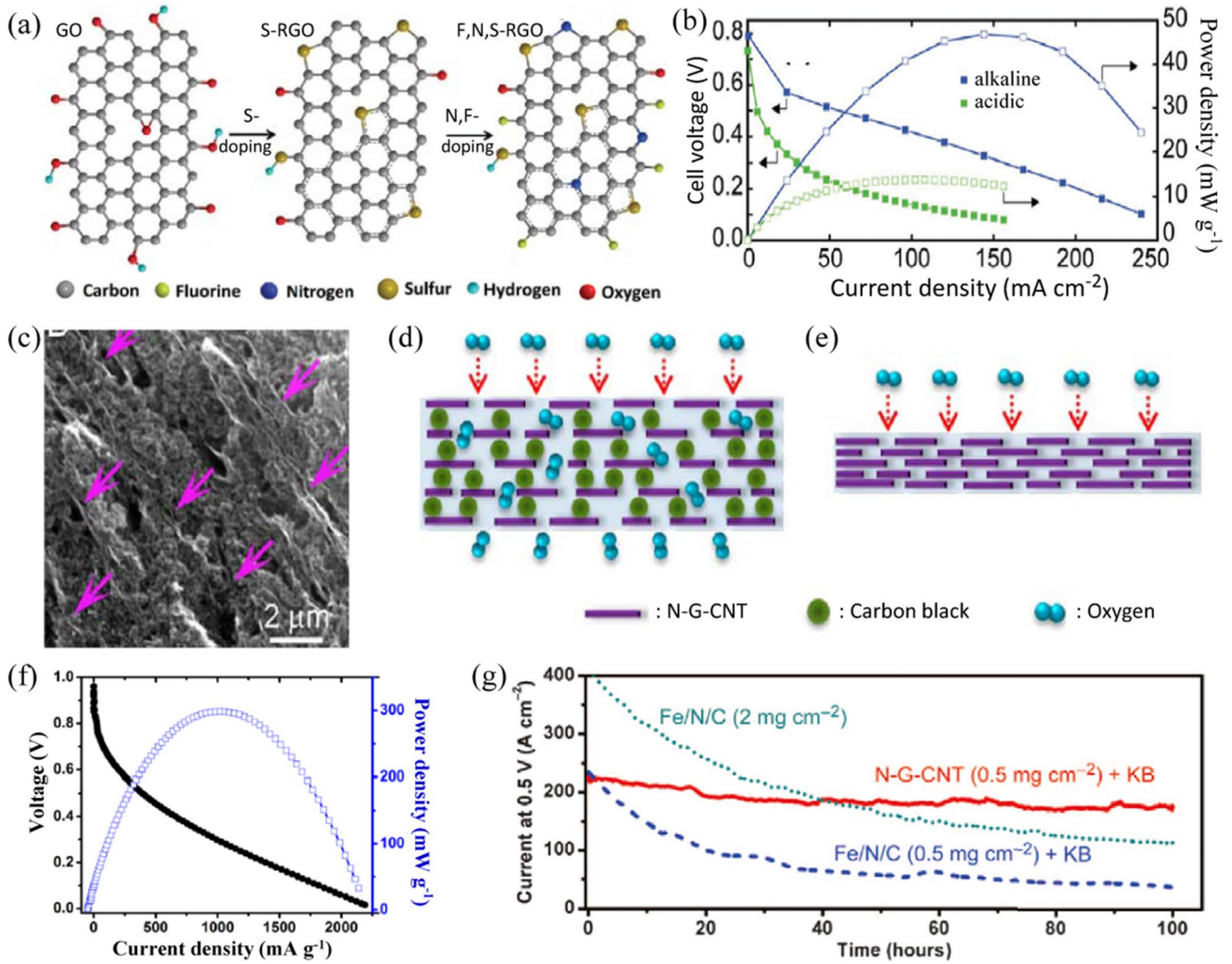

Fig. 4 **a** Schematic illustration of the hypothetical chemical structures and synthetic routes for F,N,S-rGO. Lattice defects next to S dopants and charge-polarized C-N and C-F bonds are discussed as active sites for ORR. **b** Fuel cell polarization and power density data of 5 cm^2 acidic and alkaline PEFCs with 1.5 mg cm^{-2} porous F,N,S-rGO as the cathode catalyst layer, 0.2 mg Pt-C cm^{-2} as the anode. Reproduced with permission from Ref. [17], Copyright 2017, Wiley–VCH. **c** Cross-sectional scanning electron microscope (SEM) image of the porous catalyst layer of N-G-CNT/KB/Nafion. Purple arrows indicate parallel separated N-G-CNT sheets with inter-dispersed porous CB agglomerates. Schematic drawings of O_2 efficiently diffused through (**d**) the carbon black separated N-G-CNT sheets but not (**e**) the densely packed N-G-CNT sheets. **f** Cell polarization and power density as a function of gravimetric current for N-G-CNT/KB (0.5/2 mg cm^{-2}) with the weight ratio of (N-G-CNT/KB)/Nafion = 1/1. **g** Durability of the metal-free N-G-CNT in a PEM fuel cell measured at 0.5 V compared with a Fe/N/C catalyst. Reproduced with permission from Ref. [16], Copyright 2016, AAAS

Shui et al. [16] recently demonstrated that both the VA-NCNT array and a rationally designed N-doped graphene/CNT/carbon black (Ketjenblack, KB) composite (N-G-CNT/KB) membrane electrode assembly (MEA) (Fig. 4c-e) with a well-defined porous structure exhibit excellent long-term operational stabilities and high gravimetric power densities in PEMFCs. A consistent polarization performance was observed with a peak power density over 320 W g^{-1} for the VA-NCNT MEA (Fig. 4f), outperforming or comparable to even the most active non-precious metal catalysts (i.e., Fe/N/C, Fig. 4g). Although such catalysts may accelerate the delivery of affordable and durable PEM fuel cells, the catalytic performance of carbon-based metal-free catalysts in acidic medium still requires further improvements to meet practical application requirements.

4.2 Bifunctional ORR/OER Metal-Free Catalysts for Metal-Air Batteries

Since the optimal active-site structures for different energy-related reactions (e.g., ORR, OER, and HER) are often not identical, bifunctional or multifunctional catalysts with more than one type of active sites are needed. Therefore, bifunctional metal-free carbon catalysts for ORR/OER [155, 156], OER/HER, and ORR/HER as well as tri-functional metal-free carbon catalysts for ORR/OER/HER have been developed [17, 25, 29, 155, 157–159].

Because of high theoretical energy densities, metal-air batteries have attracted ever-increasing interests for electric vehicle (EV) and hybrid electric vehicle (HEV) applications [160–162]. However, low energy efficiency, power density and short cycle life have hindered practical applications. To alleviate these problems, low-cost and efficient bifunctional ORR/OER catalysts are required. Carbon-based catalysts, possessing easily tunable structures and desirable bifunctional catalytic activities for both ORR and OER, are good selections for metal-air batteries [161]. In this section, the applications of carbon-based metal-free catalysts for Li-air batteries are highlighted, including Li-O_2 and Zn-air batteries.

4.2.1 Heteroatom-Doped Carbon for Li-Air Batteries

Doping heteroatoms into graphitic carbon structures can modify electronic and physicochemical properties of carbon materials and generate active sites for oxygen reduction [4, 29, 163–165]. Thus, heteroatom-doped carbon catalysts with desired pores are attractive for advanced Li-air batteries [166–170]. The diversity in carbon structure and morphology enables possible optimizations for gas/electrolyte diffusion and electron transport. For instance, N-doping has been demonstrated to increase catalytic activation sites for Li_2O_2 formations at carbon cathodes, thereby reducing charge overpotentials in Li-O_2 batteries [168, 169, 171, 172]. The introduction of N species into onion-like carbons can modify electron distributions to facilitate oxygen chemisorption, leading to enhanced ORR and OER kinetics, energy output, and recharging characteristics of Li-O_2 batteries [166]. N-doping of graphene has also been demonstrated to facilitate the nucleation of Li_2O_2 clusters, again leading to improved electrochemical performances [9]. Li-air batteries based on N-doped CNTs with uniform distributions of nitrogen species ensure large numbers of nucleation sites and high dispersion of discharge products, enhancing discharge capacities [173].

In addition to N-doping, other heteroatom-doping or co-doping has also been demonstrated to positively contribute to catalytic activity enhancements and cell performances. In this context, N-doping was demonstrated to contribute to discharge capacities and S-doping was verified to favor stable cycling behaviors in graphene-based Li-O_2 batteries [18]. Based on first-principles thermodynamics, Ren et al. predicted that B-doped graphene can improve charge rates of Li-air batteries and reduce O_2 evolution barriers by ca. 0.4 eV [19]. Indeed, B-doped graphene was found to provide stronger adsorption for Li_2O_2 than the pristine graphene. Thus, the introduction of B into graphene architectures can active Li-O bonds and oxidize O_2^{2-} to O_2 [20].

4.2.2 Defect and Pore Controlled Carbon Nanostructures for Li-Air Batteries

The introduction of defects into carbon materials can generate active sites for electrochemical reactions and is proven to be an effective strategy to improve catalytic activities of carbon-based materials for ORR and OER [111, 114]. Therefore, defects are also considered to be a good means to achieve the high performance in metal-air batteries. Combining theoretical and experimental studies, lattice defect sites were confirmed to play a critical role in the formation of small-sized discharge products for Li-O_2 batteries [20] in which Li_2O_2 prefers to nucleate and form near functionalized lattice defects on graphene. These isolated nanosized Li_2O_2 formations on the graphene sheet ensured smooth oxygen transport during discharge processes. Partially cracked carbon nanotubes with active edge sites and various pores have also been used as catalysts for Li-air batteries, producing an almost 2 times higher discharge capacity than raw nanotubes [174]. Generally speaking, micropores can induce high surface areas and facilitate rapid gas diffusion, ensuring a large solid–liquid–gas region, whereas mesopores can effectively improve electrode–electrolyte interactions and provide more active sites for electrochemical reactions. Macropores can reduce the blockage of electrolytes and oxygen pathways to improve O_2 diffusion and reversible conversion [175, 176]. Because discharge products, such as Li_2O_2, continuously accumulate on the surface of cathode catalysts during cycling processes, it can clog electrodes and cause electrodes to electrically disconnected. Therefore, porous carbon materials with rationally designed architectures are highly desirable as cathode materials [177], with the capacity of Li-O_2 batteries using carbon cathodes being mainly determined by the surface area, pore volume and pore size available for the deposition of discharge products [177, 178].

Hierarchically porous graphene materials consisting of microporous channels and highly connected nanoscale pores were demonstrated to deliver an exceptionally high capacity of 15,000 mAh g^{-1} in Li-O_2 batteries [20]. Here, interconnected large tunnels within a free-standing carbon nanotube film with bimodal designed hierarchically porous structure were demonstrated to facilitate continuous O_2 flow into the electrode and this nanoporosity provided ideal

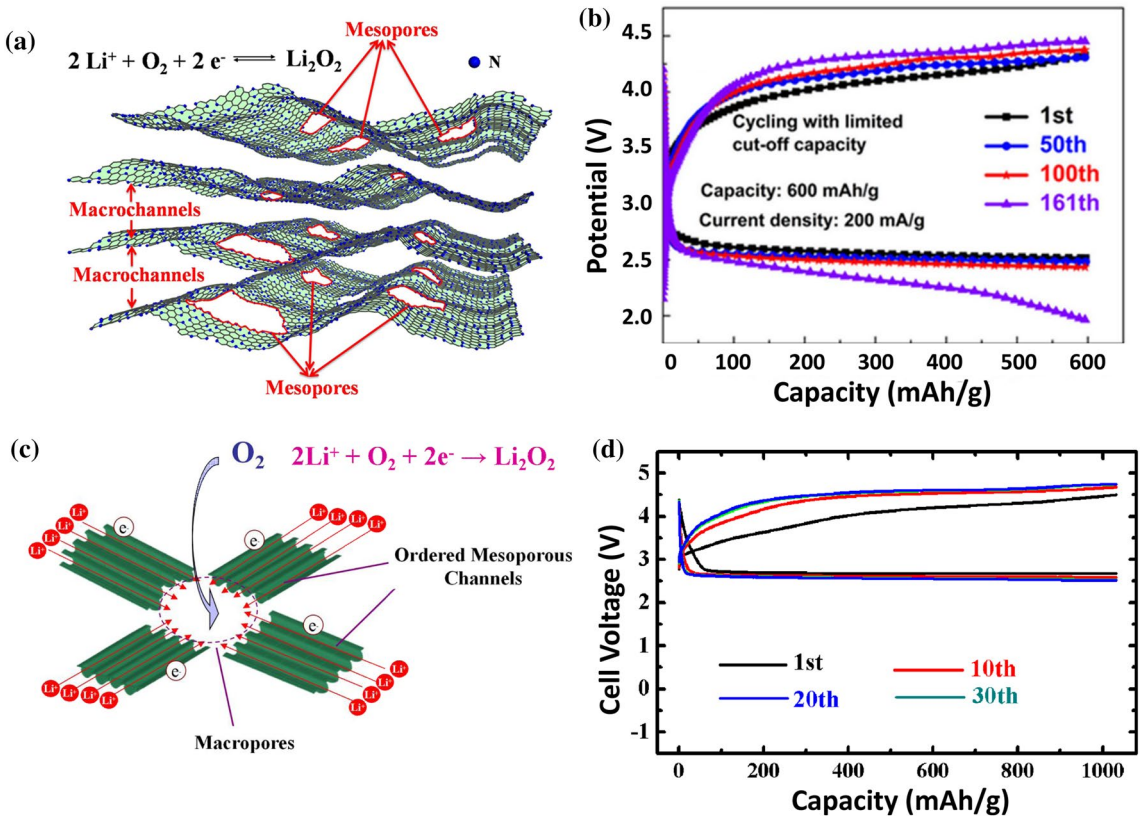

Fig. 5 **a** Schematic illustration of hierarchical carbon–nitrogen material with both macrochannels and mesopores as cathodes for Li-O_2 batteries and **b** corresponding discharge/charge profiles tested at 200 mA g^{-1}. Reprinted with permission from Ref. [21], Copyright 2014, American Chemical Society. **c** Schematic illustration of O_2/Li_2O_2 conversion in an ordered mesoporous/macroporous carbon catalyst, and **d** corresponding discharge/charge profiles tested at 250 mA g^{-1}. Reprinted with permission from Ref. [23], Copyright 2013, Wiley–VCH

triphase regions for oxygen reduction and charge storage [179]. Carbon catalysts with macropores were also proven to significantly improve electrochemical performances of Li-O_2 batteries, as confirmed by the excellent stability (up to 160 cycles) observed for Li-O_2 batteries using cathodes possessing carbon–nitrogen architectures of macrochannels and mesopores. These hierarchically structured pores can not only facilitate Li^+ diffusion and electrolyte immersion but also provide effective space for O_2 diffusion and O_2/Li_2O_2 transformation (Fig. 5a, b) [21].

Carbon-based catalysts with ordered pores have also been used to achieve high performances for Li-air batteries. For instance, Park et al. [22] employed ordered mesoporous carbon (OMC) materials as an oxygen electrode to significantly reduce charge potentials in which OMC channels can limit the size of discharge products through the confined formation of Li_2O_2. Ordered mesoporous/macroporous channels can further improve electrolyte immersion and facilitate Li^+ diffusion and electron transfer (Fig. 5c). Designed hierarchical porous architectures with macropores surrounded by ordered mesoporous channels can provide enough space for O_2 diffusion and O_2/Li_2O_2 conversion, leading to perfect cycling performance (Fig. 5d) [23].

In addition to hierarchical pores and ordered pores, 3D interconnected porous frameworks were also found to improve the performance of Li-O_2 batteries. This is because 3D frameworks provide an ideal backbone support for catalytically active sites [22]. In particular, 3D porous N-doped graphene networks constructed with interconnected nanocages possess great potential in Li-O_2 batteries [24], showing a high rate capacity of 5987 mAh g^{-1} at 3200 mA g^{-1}, and a long cycle stability of 54 cycles at 1000 mA g^{-1}. These 3D interpenetrated frameworks can not only provide multidimensional conductive networks and large areas to accommodate discharge products but can also function as "highways" for the rapid transport of O_2 and Li^+ within the entire electrode matrix.

4.2.3 Carbon-Based Bifunctional Catalysts for Zn-Air Batteries

Among all metal-air battery technologies, Zn-air battery technology is the most mature and are considered to be one of the most viable options to power electric vehicles in the future due to its high theoretical energy density (1086 Wh kg^{-1}) and low costs [180, 181]. However, the development of rechargeable Zn-air batteries has been impeded by low power output capabilities associated with a lack of satisfactory air catalysts and limited cyclabilities of Zn anodes. ORR and OER electrocatalysts have important impacts on the power density, energy efficiency, and lifetime of Zn-air batteries and much effort has been made to develop proper electrocatalysts to reduce ORR overpotentials and enhance battery discharge performances. Pt is an excellent ORR catalyst for Zn-air batteries, but it has poor OER performances and its widespread use is prohibited by its scarcity and high costs. Thus, it is crucial to explore alternative earth-abundant, low-cost, and highly effective electrocatalysts. Here, carbon-based metal-free catalysts with remarkable performances for ORR and OER, together with low costs, high corrosion resistance, and high earth abundancy, have become attractive for applications in Zn-air batteries [25, 182].

One major challenge for Zn-air batteries is to increase O_2 reduction and evolution efficiency. This requires the development of stable and effective ORR/OER bifunctional electrocatalysts that are inexpensive and stable. Based on this requirement, Dai and co-workers developed the first highly efficient Zn-air batteries (both primary and secondary) using carbon air electrodes based on N,P-doped bifunctional carbon-foam catalysts for both ORR and OER [25]. Catalysts with abundant active sites and rich O species can also facilitate oxygen adsorption and promote catalytic activities toward ORR and OER [26]. In this context, Li et al. prepared two-dimensional (2D) microporous carbon sheets with a high oxygen content that produced a small voltage gap (0.85 V) and long-term cycling stability (up to 160 h), which was superior to those of Pt/C-based Zn-air batteries [26]. The use of N-doped ORR/OER bifunctional catalysts can further improve battery performances [27], and subsequent studies have revealed that quaternary N, which provides n-type doping, is responsible for ORR and pyridinic N,

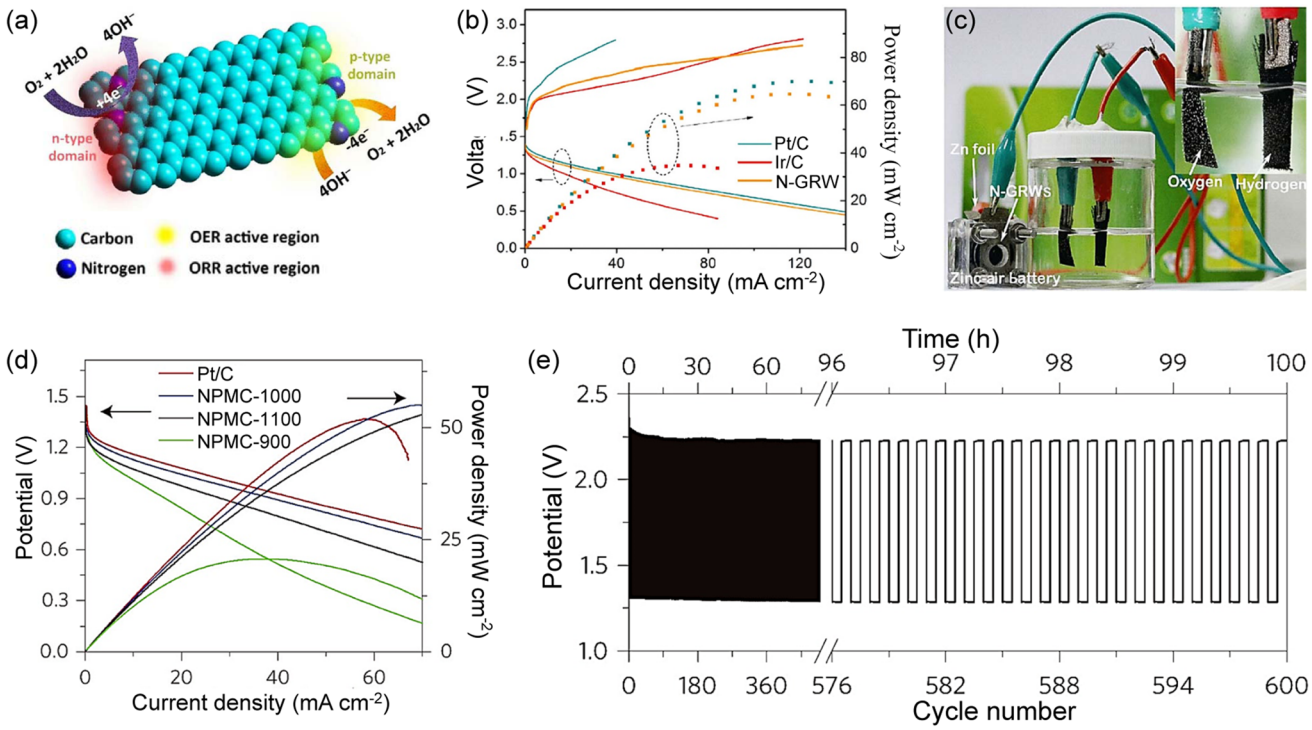

Fig. 6 **a** Schematic illustration of different active sites for ORR and OER in N-doped 3D graphene nanoribbons. **b** Discharge–charge profiles and power density plots of zinc-air batteries constructed with N-doped graphene nanoribbon networks, Pt/C, Ir/C, and mixed Pt/C + Ir/C. **c** Application of N-doped graphene nanoribbons-based Zn-air battery in powering water splitting. Reprinted with permission from Ref. [93], Copyright 2016, AAAS. **d** Polarization curves and corresponding power density plots of primary Zn-air batteries using Pt/C, N,P-doped mesoporous carbon catalysts (NPMC-900, NPMC-1000, NPMC-1100) as ORR catalysts. **e** Cycling performance of a three-electrode NPMC-1000-based Zn-air battery at 2 mA cm^{-2}. Reprinted with permission from Ref. [25], Copyright 2014, Nature Group

which provides p-type doping, can serve as active sites for OER (Fig. 6a) [93]. As a result, Zn-air batteries constructed using bifunctional N-doped 3D graphene nanoribbon air electrodes were shown to produce a peak power density of 65 mW cm^{-2} (Fig. 6b) and have been used to power splitting water units (Fig. 6c), exhibiting great potential for practical applications [93].

Compared with N-doped carbon bifunctional ORR and OER catalysts, co-doping carbon nanomaterials with different heteroatoms provide more efficient modulation of electronic properties and surface polarities to further increase ORR and OER activities. By using a N,P-doped carbon foam as the ORR/OER bifunctional catalyst, Dai and co-workers [25] developed highly efficient Zn-air batteries (Fig. 6d) in which their primary battery produced an open circuit potential of 1.48 V, a specific capacity of 735 mAh g_{Zn}^{-1} (corresponding to an energy density of 835 Wh kg_{Zn}^{-1}), a peak power density of 55 mW cm^{-2}, and sustain stable operations for 240 h after mechanical recharging. Their two-electrode rechargeable battery also cycled stably for 180 cycles at 2 mA cm^{-2}. Even at 2 mA cm^{-2}, a three-electrode rechargeable battery using their N,P-doped carbon foam produced acceptable stability (600 cycles for 100 h) (Fig. 6e) [25].

N,S-co-doped carbon was also explored as a bifunctional ORR/OER catalyst in Zn-air batteries, in which a primary Zn-air battery using a N,S-doped C_3N_4/carbon nanocrystal cathode displayed a high peak power density of 198 mW cm^{-2}, a maximum current density of 234 mA cm^{-2}, and a durability of 210 h after mechanical recharging (Fig. 7a) [28]. Furthermore, N,S-co-doped graphene microwires were used as an air cathode in a Zn-air battery and displayed a low overpotential of 0.31 V at 10 mA cm^{-2} and a high Faradic efficiency (FE) of 95% for OER [183]. In addition, this battery discharged smoothly under various current densities with a peak power density of 5.9 mW cm^{-2} at 1.1 V.

To meet the demand for flexible high-energy storage, significant efforts have also been made to develop various flexible power sources. In this regard, Liu et al. [184] prepared a nanoporous carbon nanofiber film as the air cathode in a liquid Zn-air battery and a flexible all-solid-state rechargeable Zn-air battery. The liquid Zn-air battery produced a maximum power density of 185 mW cm^{-2}, an energy density of 776 Wh kg^{-1}, a small voltage gap of 0.73 V at 10 mA cm^{-2}, and an excellent stability of up to 500 cycles. As for the flexible all-solid-state device (Fig. 7b), a low overpotential (0.78 V at 2 mA cm^{-2}) and a long cycle life (6 h) under repeated bending conditions were achieved (Fig. 7c), indicating excellent cycling performance with high mechanical stability.

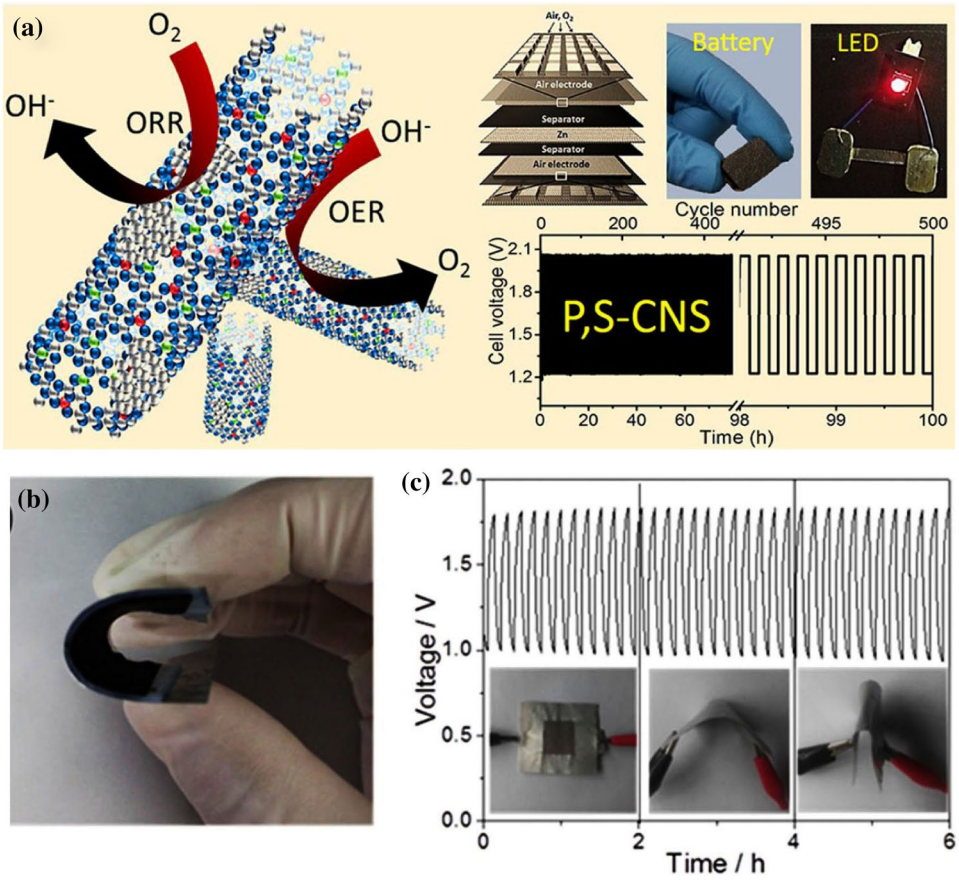

Fig. 7 **a** 3D P,S-doped carbon nitride sponge as bifunctional oxygen catalysts for Zn-air batteries. Reprinted with permission from Ref. [28], Copyright 2017, American Chemical Society. **b** Photograph of an all-solid-state nanoporous carbon nanofiber film-based Zn-air battery. **c** Cycling performance of curve at 2 mA cm^{-2} for the nanoporous carbon nanofiber film (NCNF-1000)-based all-solid-state rechargeable Zn-air battery under bending strain every 2 h. Reprinted with permission from Ref. [184], Copyright 2016, Wiley–VCH

4.3 Carbon-Based Metal-Free OER/HER Bifunctional Catalysts for Water Splitting

Water and sunlight are both renewable and readily available; therefore, sustainable energy generation from water and sunlight holds great promise in solving current energy and environmental challenges. The electrocatalytic water electrolysis reaction $H_2O \rightarrow 1/2O_2 + H_2$ consists of two half-reactions of water oxidation (i.e., OER) and proton reduction (i.e., HER), attractive for H_2 and O_2 production without the involvement of fossil fuels or the generation of greenhouse gases.

In 2013, Zhao et al. [185] first reported N-doped graphite nanomaterials that were generated from direct pyrolysis of N-rich polymers as metal-free catalysts exhibiting comparable OER catalytic activities to non-precious metal catalysts in basic mediums. Subsequently, Zheng et al. prepared C_3N_4@N-doped graphene as a metal-free electrocatalyst for sustainable and efficient H_2 production under acidic and alkaline conditions [132]. Thereafter, various heteroatom-doped carbon materials have been exploited as metal-free, active and stable OER and/or HER catalysts, as briefly described in previous reviews [4, 11].

Currently available OER electrocatalysts often show better performance in alkaline mediums than acidic electrolytes, whereas most HER electrocatalysts exhibit better performance in acidic mediums than alkaline electrolytes. This poses potential problems in situations in which HER needs to be coupled with OER in an overall water-splitting process. Therefore, it is highly desirable to develop low-cost, earth-abundant electrocatalysts to promote OER and HER simultaneously in the overall water-splitting process under the same pH environment. In this context, Davodi et al. [30] reported a facile route to prepare N-doped MWCNTs (NMWCNTs, Fig. 8a) with high activities toward OER and HER and high long-term stability.

A facile two-step method was developed to fabricate N,S-co-doped graphite foam (NSGF) from commercial graphite foils (GFL) [186], and the resultant NSGF, possessing high electrical conductivity, good flexibility, and good mechanical strength, was directly used as an electrocatalytic electrode for water oxidation. Similarly, N and F dual-doped porous graphene nanosheets (NFPGNS, Fig. 8b) have been synthesized as efficient OER/HER bifunctional metal-free electrocatalysts for overall water splitting [31]. By combining co-doping with structural regulation, 2D N,S-co-doped graphitic sheets with a unique hierarchical structure consisting of stereoscopic holes over graphitic surfaces (SHG) were developed as tri-functional catalysts for ORR, OER, and HER (Fig. 8c) [29]. The presence of stereoscopic holes ensures high surface areas with abundant interfacial active sites for electrochemical reactions. Heteroatom-doping of SHG with nitrogen and sulfur atoms can also modulate electronic and chemical characteristics to further impart functionalities. Abundant accessible active sites coupled with efficient pathways for electron and electrolyte/reactant transport allow the newly developed SHG to be applied as an efficient metal-free ORR/OER/HER tri-functional catalyst with long-term stability in alkaline electrolytes, and its applications as a multifunctional catalyst were demonstrated in a water-splitting device [29].

Aside from these N-doped, N,F- or N,S-co-doped carbon-based OER/HER bifunctional catalysts for water splitting, a N,O-co-doped porous carbon OER/HER bifunctional catalyst was prepared by pyrolyzing a metal–organic framework (MOF); such as zeolitic imidazolate framework-8 (ZIF-8), followed by H_2SO_4 modulation (Fig. 8d), and demonstrated high performances for water splitting with a current density of 10 mA cm^{-2} over 8 h under a potential of 1.82 V and a faraday efficiency (FE) of 98.0–99.1% in 0.1 M KOH electrolyte [187]. N,P,O-tri-doped porous graphite carbon@oxidized carbon cloth (donated as: PGC/OCC) has also been developed for overall water splitting with a low overpotential of 410 mV, a current density of 10 mA cm^{-2}, a small Tafel slope of 83 mV dec^{-1}, and a long-term electrochemical durability [158]. Impressively, this 3D porous carbon cloth catalyst showed not only high catalytic performances in alkaline water electrolyzers (10 mA cm^{-2} at a cell voltage of 1.66 V) but also superior catalytic activity and stability under both strongly acidic and neutral conditions. This observed excellent HER and OER catalytic performance was attributed to the high conductivity of graphitized carbon, the unique 3D porous architecture between PGC and OCC, and the presence of electron-rich phosphorus and nitrogen dopants. Another carbon-based metal-free OER/HER bifunctional catalyst for high-performance water splitting is defect-rich porous carbon (DRPC) prepared using a template approach. This catalyst was also used for self-powered electrochemical water splitting (Fig. 8e-g) to demonstrate its great potential for practical applications [188].

4.4 Carbon-Based Metal-Free ORR-OER-HER Tri-functional Catalysts for Integrated Energy Devices

Chemical energy in the form of H_2 can be generated by splitting water, which in turn can be used in fuel cells to produce clean electricity to meet growing energy demands. For this purpose, the low-cost production of H_2 through water splitting by either the direct use of sunlight for photocatalytic water splitting or through electricity generated from photovoltaic devices for photoelectrochemical water splitting is essential. Through photocatalytic and/or photoelectrochemical water splitting, clean electricity can be continuously generated from water and sunlight by simply feeding fuel cells with hydrogen and oxygen gases from water splitting to produce electricity with water being the only by-product.

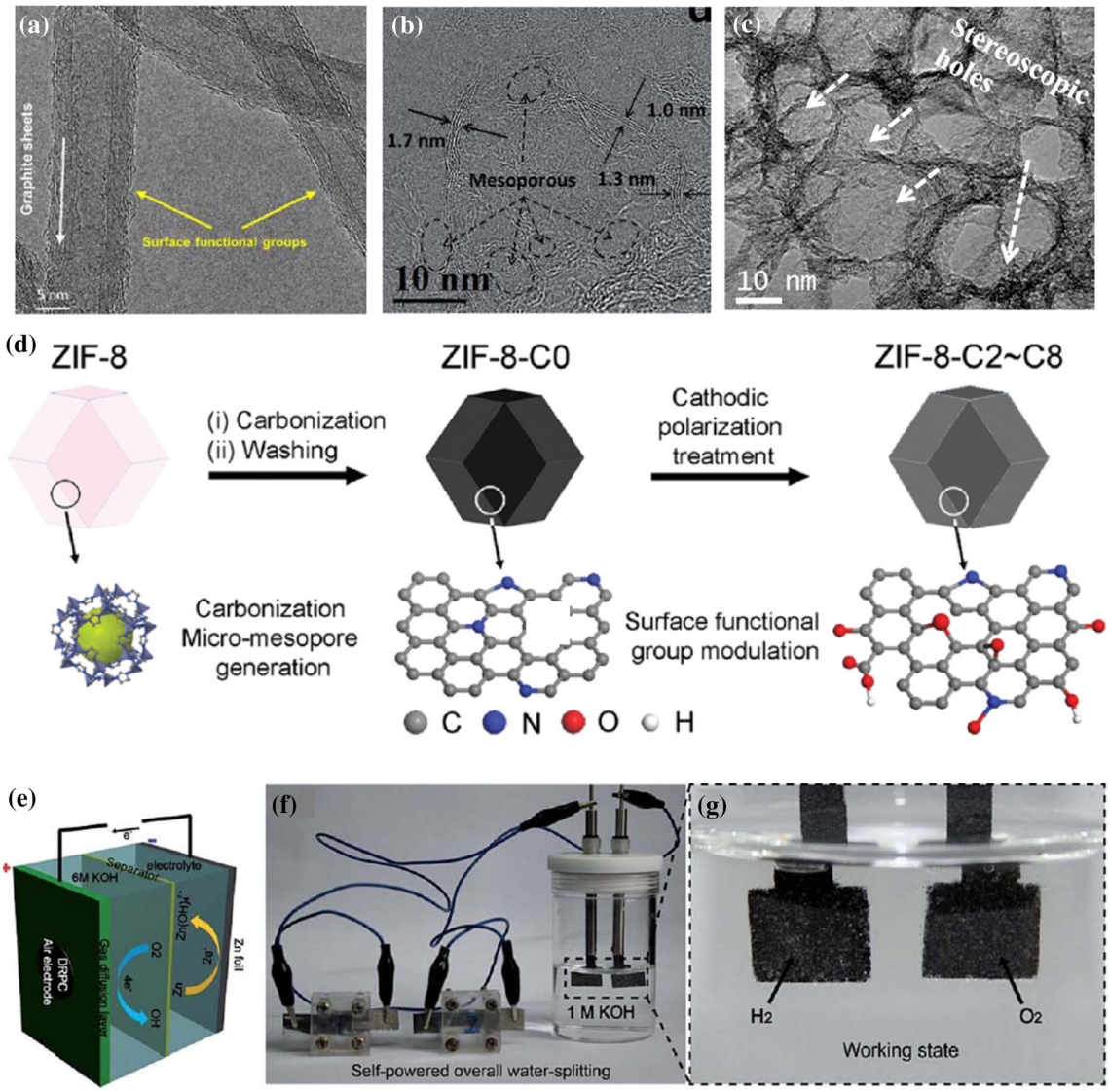

Fig. 8 **a** HR-TEM image of N-doped MWCNTs. Reprinted with permission from Ref. [30], Copyright 2017, Elsevier. **b** TEM image of N and F dual-doped porous graphene nanosheets (NFPGNS). Reprinted with permission from Ref. [31], Copyright 2017, Royal Society of Chemistry. **c** TEM of the 2D N,S-co-doped graphitic sheets with a unique hierarchical structure consisting of stereoscopic holes over the graphitic surface (SHG) as tri-functional catalysts for ORR, OER, and HER. Reprinted with permission from Ref. [29], Copyright 2017, Wiley–VCH. **d** Schematic illustration of the synthesis of N,O-co-doped porous carbon from ZIF-8. Reprinted with permission from Ref. [187], Copyright 2017, Royal Society of Chemistry. **e** Schematic illustration of the two-electrode Zn-air battery. **f**, **g** A photograph showing an alkaline water-splitting electrolyzer powered by two Zn-air batteries (**f**) and the electrocatalytic evolution of hydrogen and oxygen bubbles (**g**). Reprinted with permission from Ref. [188], Copyright 2017, Royal Society of Chemistry

The water by-product can then be reused for photocatalytic/photoelectrochemical water splitting to maintain the whole cycle for renewable generation of clean electricity. To realize this ideal energy cycle, efficient catalysts are required for HER, OER, and ORR.

By rationally designing N,S-co-doped porous graphitic networks with cross-linked three-dimensional (3D) structures (N,S-3DPG), Dai and co-workers have developed a low-cost, highly efficient tri-functional catalyst to simultaneously catalyze HER, OER, and ORR in alkaline electrolytes [189]. The unusual tri-functional electrocatalytic performance of N,S-3DPG is attributed to synergistic effects arising from N,S-co-doping and unique 3D porous network structures [4, 89, 190]. Based on the newly developed ORR/OER/HER tri-functional catalyst from earth-abundant carbon materials, an integrated energy system was devised in which assembled perovskite solar cells were used for photoelectrochemical water splitting (OER and HER) to produce hydrogen and oxygen gases for fuel cells (ORR) to renewably generate clean electricity. This system represents a new

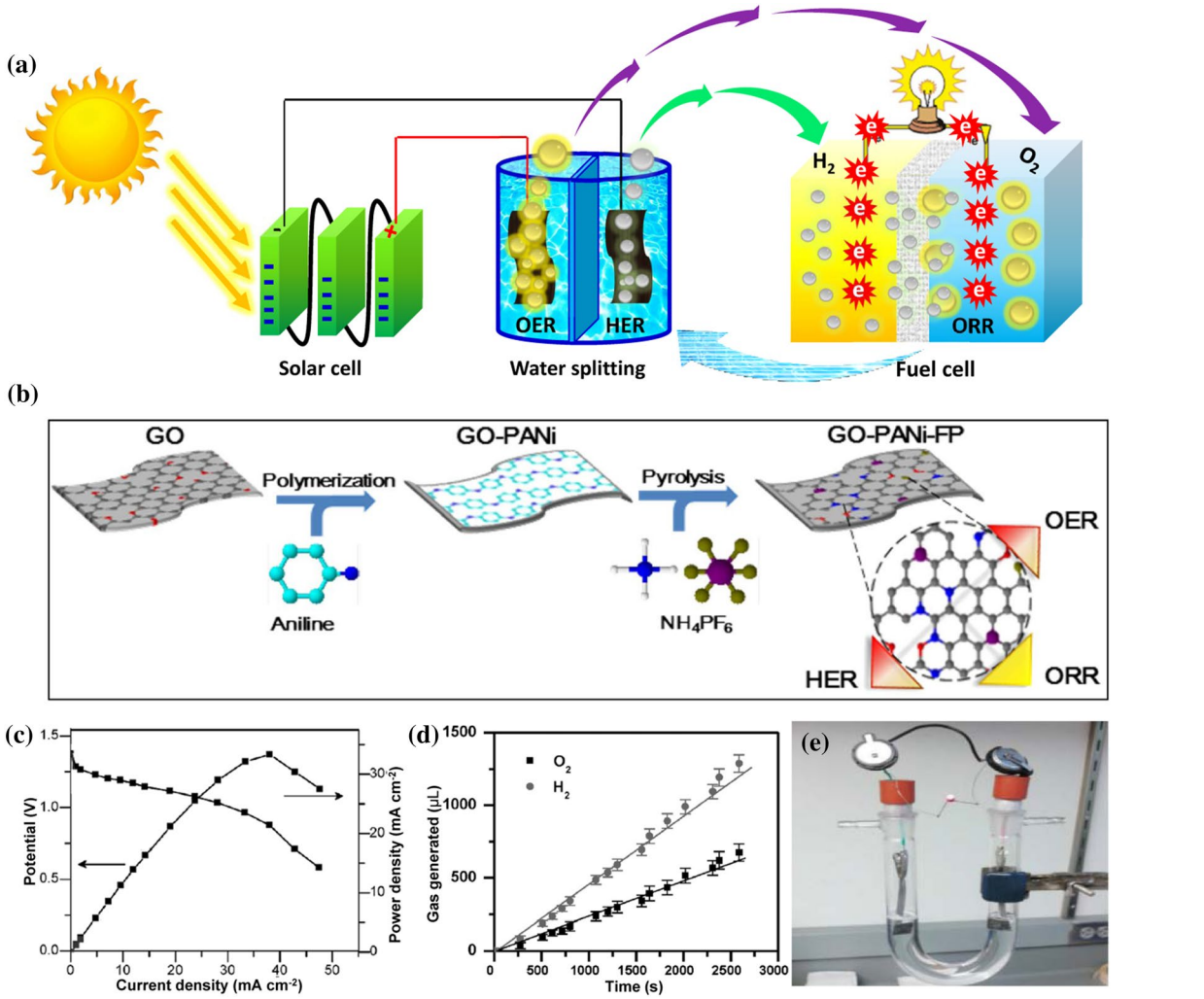

Fig. 9 **a** Schematic illustration of a multifunctional hybrid energy device of perovskite cells assembled with a water-splitting device and a fuel cell. Reprinted with permission from Ref. [189], Copyright 2017, Elsevier. **b** The preparative process for the synthesis of GO-PANi-FP tri-functional electrocatalyst. **c** Polarization and power density curves of Zn-air batteries using N,P, F-tri-doped graphene as ORR/OER catalyst. **d** O_2 and H_2 production volumes as a function of water-splitting times, using the same N,P, F-tri-doped graphene as the OER/HER bifunctional catalyst. **e** A water-splitting device powered by Zn-air batteries. Reprinted with permission from Ref. [155], Copyright 2016, Wiley–VCH

conceptually important approach to cost-effective generation of clean and renewable electricity from sunlight and water (Fig. 9a) [189].

Recently, metal-free photocatalysts based on carbon dots/g-C_3N_4 have been reported [191]. Lee and co-workers [191] found that a very small loading of carbon dots (0.0016 wt%) embedded in the matrix of g-C_3N_4 can lead to stable overall water splitting to H_2 and O_2 in a stoichiometric ratio under visible light for at least 200 days. Remarkably, a solar-to-hydrogen yield of 2% was obtained with a carbon dot loading of 0.48 wt% under AM 1.5G solar simulation [191].

Through a facile procedure to remove nitrogen from a N-doped precursor, Yao and co-workers [121] developed high-performance defect-induced tri-functional carbon catalysts for ORR, OER, and HER. Zhang et al. [155], also prepared a high-performance ORR/OER/HER tri-functional metal-free catalyst through in situ tri-doping of a self-assembled graphene foam with N, P, and F (Fig. 9b). The resultant N,P,F-tri-doped graphene foam was tested as an OER/HER bifunctional catalyst for oxygen and hydrogen gas production in an electrochemical water-splitting unit that was powered by an integrated Zn-air battery based on an air electrode made from the same electrocatalyst for ORR (Fig. 9c-e) [155]. Although recent studies have demonstrated the feasibility of constructing integrated energy systems of (photo)electrochemical or

even photocatalytic water splitting coupled with fuel cells, practical applications are still not within reach.

4.5 Carbon-Based Metal-Free Catalysts for Solar Cells and Metal-I_2 Batteries

The over use of fossil fuels with intrinsically associated greenhouse effects has made it more important now than ever to develop clean and renewable energy technologies. Solar cells, especially dye-sensitized solar cells (DSSCs), are cost-effective, environmentally friendly, and highly efficient energy conversion systems. Thus, solar cells are of vital importance among all other green and renewable energy technologies [192, 193]. A conventional DSSC is composed of a photoanode sensitized by a dye, an electrolyte containing a redox couple (e.g., triiodide/iodide), and a Pt-based counter electrode (CE) [193]. As alternatives for Pt-based catalysts, metal-free heteroatom-doped carbon catalysts have been demonstrated to be effective at catalyzing the reduction of I_3^- to I^- in DSSCs [32, 33]. In particular, defective graphene sheets with oxygen-contained functional groups have been demonstrated to exhibit comparable energy conversion efficiency (5.0%) to Pt (5.5%) (Fig. 10a, b) [32]. A DSSC with a 3D N-doped graphene foam cathode can displayed a power conversion efficiency of 7.07%, comparable to its counterpart based on a Pt cathode (7.44%) (Fig. 10c, d) [33].

Like graphene-based catalysts, defective CNT microballs have also been used to replace Pt-based cathodes in DSSCs to achieve remarkable energy conversion efficiencies of about 7% [34, 35]. Of particular interest, a free-standing vertically aligned N-doped CNT array, instead of randomly oriented CNTs, has also been used as a counter-electrode catalyst in DSSCs to exhibit a high power conversion efficiency of 7.04%, which is close to that of conventional Pt counter electrodes [194]. A vertically

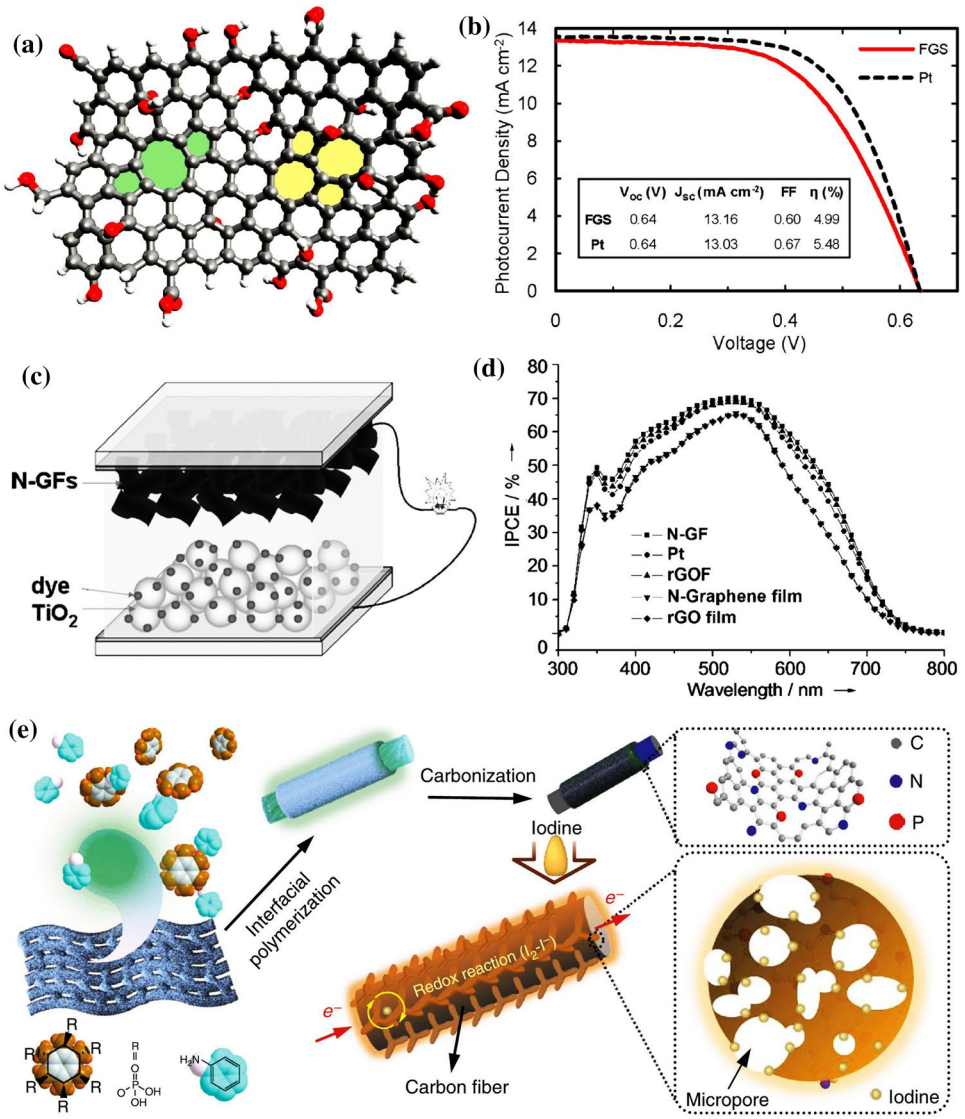

Fig. 10 **a** Schematic of functional groups and lattice defects (green and yellow) on a functional graphene sheet (FGS). Gray: Carbon atoms; red: oxygen atoms; white: hydrogen atoms. **b** Current density/voltage curves of FGS-based DSSCs. Active area: 0.39 cm^2. Reproduced with permission from Ref. [32], Copyright 2010, American Chemical Society. **c** A DSSC based on a 3D N-doped graphene foam (N-GF) cathode and **d** the corresponding incident photon to charge carrier efficiency (IPCE) in comparison with Pt, rGOF, N-graphene film, and rGO film. Reproduced with permission from Ref. [33], Copyright 2012, Wiley–VCH. **e** Preparation of N,P-doped hierarchical porous carbon matrix (HPMC-NP) and the loading of iodine. Reprinted with permission from Ref. [197], Copyright 2017, Nature Group

aligned SWCNT array also displayed a high conversion efficiency of 5.5%, comparable to 5.6% obtained with a Pt-based DSSC tested under the same conditions [195]. In addition, carbon catalysts comprised of CNTs coated onto a flexible graphene paper achieved 83% conversion efficiency of that of a Pt electrode [196].

In addition to solar cells, the redox reactions of iodine also play a vital role in Li/Na-I_2 batteries. However, the development of economically efficient and highly conducting iodine-based cathodes with stable and high iodine loading is challenging [197]. Several carbon hosts, including carbon black [198], nanoporous carbon [199], vertically aligned carbon nanotubes [200], and porous carbon microtubes [201], have been employed to load I_2 for Li-I_2 batteries.

Inspired by the excellent electrocatalytic activities induced by heteroatom-doping for metal-air batteries [25, 202] and its significant effects on enhancing capacity and cycling stability of Na/Li-ion batteries [203], Lu et al. [197] used hierarchical porous N,P-co-doped carbon matrixes as hosts for I_2 loading in I_2-based batteries (Fig. 10e). Here, high discharge capacities of 386 and 253 mAh g^{-1} with good stabilities up to 2000 cycles and 500 cycles were achieved for Li-I_2 and Na-I_2 batteries, respectively, based on iodine-containing cathodes. Excellent reversible capacities with good capacity retentions (e.g., 76.7% after 500 cycles and 69.8% after 300 cycles at 500 mA g^{-1}) were also obtained even for Li-I_2 and Na-I_2 batteries with I_2-contained hierarchical porous N,P-doped carbon matrix cathodes and hierarchical porous N,P-doped carbon matrix anodes.

4.6 Carbon-Based Metal-Free Catalysts for CO_2 Reduction and Li-CO_2 Batteries

Rapidly increasing CO_2 concentrations around the globe has resulted in numerous environmental issues, such as global warming, ocean acidification, polar ice melting, sea level rising, and species extinction [204]. CO_2 capture and conversion is considered to be an effective means to minimize atmospheric CO_2 by converting CO_2 into cost-effective carbon-containing fuels [205, 206]. In this context, carbon-based metal-free catalysts have also been used for CO_2RR. Figure 11 and Table 1 represent recent advances in the development of carbon-based metal-free catalysts for CO_2RR [36, 37, 207–214].

As seen in Fig. 11, metal-free carbon catalysts based on N-doped carbon nanofibers (NCNFs) generated from the electrospinning of polyacrylonitrile (PAN) was first reported in 2013 for CO_2RR [36]. Subsequently, N-doped CNTs (NCNTs) were demonstrated to be highly active, selective, and stable catalysts for the electrocatalytic reduction of CO_2 to CO [37–40]. Combined XPS analyses and DFT calculations indicate that pyridinic N plays an important role in CO_2RR, whereas for graphitic N, electrons are localized in the π antibonding orbital, becoming less accessible for CO_2 binding. Pyrrolic N is believed to

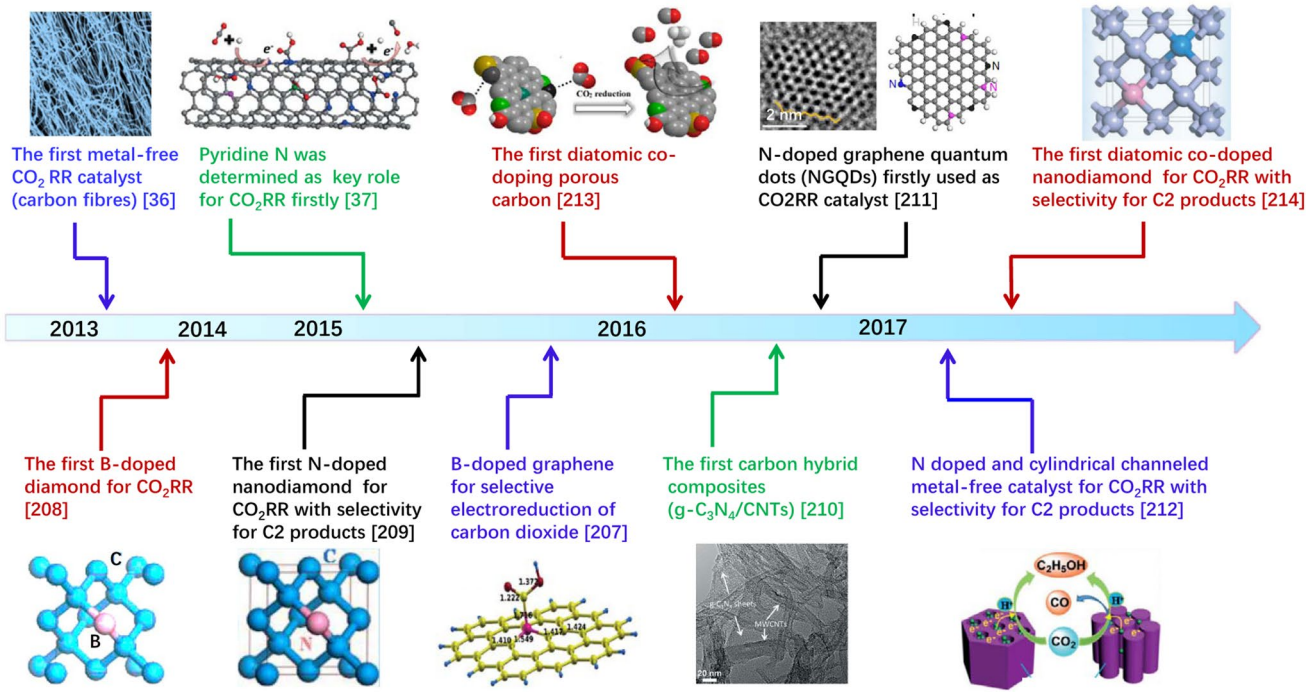

Fig. 11 Timeline showing important developments in metal-free carbon-based catalysts for CO_2RR

Table 1 Comparison of materials, preparation methods, specific performances, and characteristics of reported metal-free carbon-based catalysts for CO_2RR

Samples	Preparation methods	Performance	Characteristics	References
N-doped carbon fibers	Electrospinning and carbonization	An order of magnitude higher current density compared with silver catalysts	The first metal-free carbon-based catalyst for $RRCO_2$	[36]
B-doped diamond	Microwave plasma-assisted chemical vapor deposition	High FE (74%) for formaldehyde production	The first B-doped diamond catalyst for CO_2RR	[208]
N-doped carbon nanotubes	Liquid chemical vapor deposition	Conversion selectivity of CO_2 to CO can reach 80%	With large amounts of pyridinic N active sites	[37]
N-doped diamond	Photolithography and deposition	Converts CO_2 to acetate with an onset potential of − 0.36 V	Good selectivity for converting CO_2 to acetate over formate	[209]
B-doped graphene	Pyrolysis	Current remains at least 3 times higher than that of graphene electrodes	Reveal mechanistic details of CO_2 adsorption and subsequent conversion to formic acid/formate	[207]
Nanometre-size N-doped graphene quantum dots	Exfoliating and cutting graphene oxide	A high total FE of carbon dioxide reduction of up to 90%, with selectivity for ethylene and ethanol conversions reaching 45%	Generates C_2 and C_3 production	[211]
N-doped mesoporous carbon	Template method	Efficient production of ethanol with nearly 100% selectivity and high FEof 77% at − 0.56 V	Synergetic effects of N-doping and cylindrical channel configurations facilitate superior electrocatalytic performance for synthesizing ethanol	[212]
B,N-co-doped nanodiamond	Hydrothermal process and electrodeposition	Ethanol selectivity achieved on BND with a high FE of 93.2% (− 1.0 V)	The first co-doped nanodiamond for CO_2RR	[214]

have minimal impacts on CO_2RR. This is because pyrrolic N atoms are often located toward the center of the carbon framework, making it difficult for lone pairs of pyrrolic N to be accessible for CO_2 binding. N-doped graphene (NG) electrocatalysts have also been demonstrated to show robust electrocatalytic activities toward CO_2RR [38, 215]. Particularly, N-doped graphene-like carbon materials (NGMs) were reported to be highly efficient electrocatalysts for CO_2RR in ionic liquid electrolytes (e.g., 1-butyl-3-methylimidazolium tetrafluoroborate, [BMIM]BF_4) to produce CH_4 as the main product with a FE as high as 93.5% and a more than 6 times higher current density than metal Cu-based catalysts [216].

Along with N-doped carbon fibers and CNTs, boron-doped graphene (BG) has also been studied for the reduction of CO_2 to formate [207]. Even boron-doped diamonds (BDD) have been demonstrated to show promising catalytic activity for the reduction of CO_2 to methanol, despite diamonds being often considered chemically inert [208]. Here, it was found that sp^3-bonded carbons on BDD can act as active sites for CO_2RR. Because C2 products are more valuable than C1 products, the development of efficient carbon electrocatalysts for the reduction of CO_2 to C2 products is highly desirable. N-doped diamonds (NDD) can serve as promising electrocatalysts for CO_2 reduction to not only C1 products (formate), but also C2 products (acetate) with high efficiency, fast kinetics, and good selectivity [209]. The higher production rates for acetate than formate on NDD catalysts indicate that C–C coupling preferentially occurs at the initial stage of CO_2RR. Co-doping was also found to enhance CO_2 reduction. Here, B,N-co-doped diamonds (BND) were found to be efficient and stable electrodes for the selective reduction of CO_2 to ethanol [214] in which B- and N-doping regulates the electronic structure of the diamond [217, 218] through synergistic effects to convert CO_2 into highly reduced C2 products (i.e., CH_3CH_2OH). N,S-co-doped polymer-derived carbon (CPSN) was also demonstrated to be an electrocatalyst for CO_2RR; producing a higher FE than S-doped polymer-derived carbons (CPS), with positively charged carbon atoms in the vicinity of pyridinic N- and/or S-heteroatoms being main active sites [213].

Much like carbon catalysts for other electrocatalytic reactions discussed above, 3D architectures and topological defects also play important roles in regulating CO_2 reduction. For example, graphitic carbon nitride/carbon nanotube composites (g-C_3N_4/CNT), displaying good catalytic performances for CO_2RR to CO with a maximum FE of 60% at an applied potential of − 0.75 V, can attribute its high catalytic activity to the N-doping, high specific surface area (123.4 $m^2\ g^{-1}$), and high electrical conductivity of CNTs [210]. In an independent study, a binder-free N-doped nanoporous carbon/CNT (HNCM-CNT) composite electrode was also demonstrated to show high activity, selectivity, and stability for formate production from CO_2, achieving a high FE of 81% [219].

With rich topology and edges [211], N-doped graphene quantum dots (NGQDs) were reported as active metal-free electrocatalysts for CO_2RR with high reduction current densities at low overpotentials. By regulating the applied potential, CO_2 can be reduced on NGQDs into a series of species ranging from C1 to C3 products. Recent studies confirm that products from CO_2RR can be controlled by structure configurations of N-doped carbon-based catalysts. A class of mesoporous and inverse mesoporous N-doped carbons with highly uniform cylindrical channels were subsequently developed to dramatically boost C–C bond formations in CO_2 electroreductions [212]. The uniformly distributed pyridinic/pyrrolic N sites on the inner surface of the cylindrical channels efficiently supply electrons necessary for the dimerization of CO* intermediates to produce ethanol.

Similar to the use of bifunctional carbon catalysts for metal-air batteries [220], Qie et al. found that B,N-doped holey graphene (HG) bifunctional catalysts can effectively increase discharge capacities, reduce charge/discharge overpotentials, and significantly improve the cycle stability of Li-CO_2 batteries, as shown in Fig. 12a, b [41]. Using carbon nanotubes as an active air cathode, Hu et al. [42] successfully constructed a flexible Li-CO_2 battery (Fig. 12c) using a poly(methacrylate)/poly(ethylene glycol)-$LiClO_4$-3wt%SiO_2/porous CNT cathode which exhibited a good cycling life up to 100 cycles and a long operation time of 220 h at 55 °C. This cell retained satisfactory cycling performance even under different degrees of bending (Fig. 12d).

The electrochemical reduction of CO_2 to more reduced organic feedstocks (e.g., HCOOH, CH_3OH, C_2H_4, CH_4, CO) is a promising method to store energy from intermittent electricity sources (i.e., wind and solar) and synthesize carbon-based compounds from CO_2 through carbon fixation. Compared with CO_2RR using metal-based electrocatalysts [221] however, CO_2RR using metal-free carbon-based electrocatalysts still require further development. Continued research efforts in this growing field will lead to eventual commercialization, allowing for both efficient energy storage and environmental protection.

5 Concluding Remarks

Upon doping of heteroatoms and/or introduction of defects into carbon networks, graphitic carbon materials exhibit interesting catalytic properties that are attractive for eco-friendly electrochemical energy conversion and storage applications, including water-splitting, dye-sensitized solar cells, metal-air batteries, fuel cells, and carbon dioxide reductions. The combination of photocatalytic/photoelectrochemical water splitting for on-site generation of O_2 and

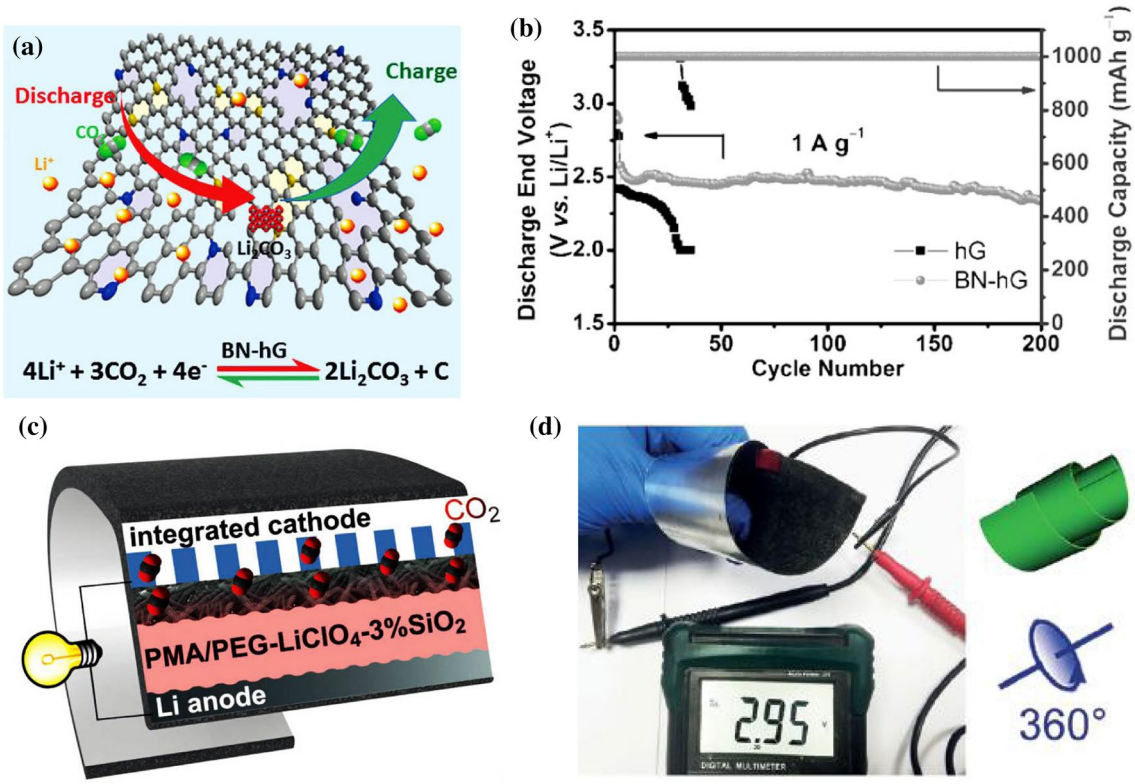

Fig. 12 **a** B,N-doped holey graphene applied in Li-CO_2 batteries and **b** long-term cycling performance of holey graphene (hG) and BN-doped hG-based Li-CO_2 batteries. Reproduced with permission from Ref. [41], Copyright 2017, Wiley–VCH. **c** Schematic illustration of Li-CO_2 batteries with a liquid-free composite polymer electrolyte (CPE)@CNTs cathode and **d** constructed Li-CO_2 batteries twisting to 360°. Reproduced with permission from Ref. [42], Copyright 2017, Wiley–VCH

H_2 gases with H_2-O_2 fuel cells creates a cost-effective and H_2-storage-free approach toward the renewable generation of clean electricity from sunlight and water. Sustainable energy generation from water and sunlight holds great promise as a solution to current energy and environmental challenges. However, low-cost but efficient catalysts are required. Recent developments in carbon nanomaterials with various architectures offer opportunities for the development of advanced carbon-based catalysts with multifunctionalities. The introduction of heteroatoms (e.g., N) and/or defects into graphitic carbon nanomaterials has been demonstrated to cause electron modulation to provide desirable electronic structures for many catalytic processes, including ORR, OER, HER, triiodide reduction, and CO_2RR. Although numerous progresses have been achieved, there are still many challenges that must be overcome in order for carbon-based catalysts to replace metal-based counterparts in commercial applications.

In most cases, the exact catalytic role and location of heteroatoms in carbon-based catalysts are still not fully understood, and long-term durability, particularly in practical devices, has not been tested with standard evaluation protocols. Difficulties in determining active-site structures hinder efforts to precisely control active sites and hence electrocatalytic performance. Therefore, new synthetic and/or doping strategies must be developed to precisely control the location, content, and distribution of dopants in heteroatom-doped carbon catalysts. The development of in situ, real-time characterization techniques is also important to probe the nature of active sites and to understand electrocatalytic mechanisms. Combined experimental and theoretical approaches are crucial as computer simulations and calculations have been proven to be powerful tools in the search for active centers and the study of the basic sciences behind electrocatalysis. In addition to further studies into catalytic mechanisms and kinetics, long-term performance evaluations of metal-free carbon-based catalysts in various actual devices need to be performed. For industrial applications, the development of facial and cost-effective methods for large-scale production of carbon nanomaterials with well-defined structures and catalytic properties is essential. With the large number of carbon catalysts already reported and more to be developed, the possibility of producing multifunctional carbon-based metal-free catalysts with exotic electrocatalytic properties suitable for a wide range of energy devices and environmental protection systems can soon be achieved. Continued research and

development in this exciting field will overcome major hurdles faced by carbon catalysts for energy conversion and storage and environmental protection, leading to better fuel economy, decreased harmful emissions, and reduced reliance on petroleum sources.

Acknowledgements We would like to thank our colleagues for their contributions to the works cited. We are also grateful for the financial support from NSF (CMMI-1400274, DOD-AFOSR-MURI (FA9550-12-1-0037), NASA (NNX16AD48A, NNC16CA42C), the Key Program of the National Natural Science Foundation of China (51732002), the National Key Research and Development Program of China (2017YFA0206500), the Distinguished Scientist Program at BUCT (buctylkxj02), and the National Basic Research Program of China (2011CB013000).

References

1. Dunn, B., Kamath, H., Tarascon, J.M.: Electrical energy storage for the grid: a battery of choices. Science **334**, 928–935 (2011)
2. Lewis, N.S., Nocera, D.G.: Powering the planet: chemical challenges in solar energy utilization. Proc. Natl. Acad. Sci. USA **103**, 15729–15735 (2006)
3. Zhang, J., Xia, Z., Dai, L.: Carbon-based electrocatalysts for advanced energy conversion and storage. Sci. Adv. **1**, e1500564 (2015)
4. Dai, L., Xue, Y., Qu, L., et al.: Metal-free catalysts for oxygen reduction reaction. Chem. Rev. **115**, 4823–4892 (2015)
5. Hu, C., Xiao, Y., Zhao, Y., et al.: Highly nitrogen-doped carbon capsules: scalable preparation and high-performance applications in fuel cells and lithium ion batteries. Nanoscale **5**, 2726–2733 (2013)
6. Xue, Y., Ding, Y., Niu, J., et al.: Rationally designed graphene-nanotube 3D architectures with a seamless nodal junction for efficient energy conversion and storage. Sci. Adv. **1**, 1400198 (2015)
7. Kumar, B., Asadi, M., Pisasale, D., et al.: Renewable and metal-free carbon nanofibre catalysts for carbon dioxide reduction. Nat. Commun. **4**, 2819 (2013)
8. Zhang, J., Qu, L., Shi, G., et al.: N, P-codoped carbon networks as efficient metal-free bifunctional catalysts for oxygen reduction and hydrogen evolution reactions. Angew. Chem. Int. Ed. **55**, 2230–2234 (2016)
9. Shui, J., Lin, Y., Connell, J., et al.: Nitrogen-doped holey graphene for high-performance rechargeable Li-O_2 batteries. ACS Energy Lett. **1**, 260–265 (2016)
10. Liu, X., Dai, L.: Carbon-based metal-free catalysts. Nat. Rev. Mater. **1**, 16064 (2016)
11. Hu, C., Dai, L.: Carbon-based metal-free catalysts for electrocatalysis beyond the ORR. Angew. Chem. Int. Ed. **55**, 11736–11758 (2016)
12. Dai, L.: Carbon-based catalysts for metal-free electrocatalysis. Curr. Opin. Electrochem. **4**, 18–25 (2017)
13. Lai, L.F., Potts, J.R., Zhan, D., et al.: Exploration of the active center structure of nitrogen-doped graphene-based catalysts for oxygen reduction reaction. Energy Environ. Sci. **5**, 7936–7942 (2012)
14. Li, Q.F., He, R.H., Jensen, J.O., et al.: Approaches and recent development of polymer electrolyte membranes for fuel cells operating above 100 C. Chem. Mater. **15**, 4896–4915 (2003)
15. Zhang, H.W., Shen, P.K.: Recent development of polymer electrolyte membranes for fuel cells. Chem. Rev. **112**, 2780–2832 (2012)
16. Shui, J., Wang, M., Du, F., et al.: N-doped carbon nanomaterials are durable catalysts for oxygen reduction reaction in acidic fuel cells. Sci. Adv. **1**, e1400129 (2015)
17. Pham, C., Klingele, M., Britton, B., et al.: Tridoped reduced graphene oxide as a metal-free catalyst for oxygen reduction reaction demonstrated in acidic and alkaline polymer electrolyte fuel cells. Adv. Sustain. Syst. **1**, 1600038–1600047 (2017)
18. Han, J.H., Guo, X.W., Tto, Y., et al.: Effect of chemical doping on cathodic performance of bicontinuous nanoporous graphene for Li-O_2 batteries. Adv. Energy Mater. **6**, 1501870 (2016)
19. Ren, X., Zhu, J., Du, F., et al.: B-doped graphene as catalyst to improve charge rate of lithium-air battery. J. Phys. Chem. C **118**, 22412–22418 (2014)
20. Xiao, J., Mei, D., Li, X., et al.: Hierarchically porous graphene as a lithium-air battery electrode. Nano Lett. **11**, 5071–5078 (2011)
21. Zhang, Z., Bao, J., He, C., et al.: Hierarchical carbon-nitrogen architectures with both mesopores and macrochannels as excellent cathodes for rechargeable Li-O_2 batteries. Adv. Funct. Mater. **24**, 6826–6833 (2014)
22. Park, J.B., Lee, J., Yoon, C.S., et al.: Ordered mesoporous carbon electrodes for Li-O_2 batteries. ACS Appl. Mater. Interfaces **5**, 13426–13431 (2013)
23. Guo, Z., Zhou, D., Dong, X.L., et al.: Ordered hierarchical mesoporous/macroporous carbon: a high-performance catalyst for rechargeable Li-O_2 batteries. Adv. Mater. **25**, 5668–5672 (2013)
24. Zhao, C., Yu, C., Liu, S., et al.: 3D porous N-doped graphene frameworks made of interconnected nanocages for ultrahigh-rate and long-life Li-O_2 batteries. Adv. Funct. Mater. **25**, 6913–6920 (2015)
25. Zhang, J., Zhao, Z., Xia, Z., et al.: A metal-free bifunctional electrocatalyst for oxygen reduction and oxygen evolution reactions. Nat. Nanotechnol. **10**, 444–452 (2015)
26. Li, B., Geng, D., Lee, X.S., et al.: Eggplant-derived microporous carbon sheets: towards mass production of efficient bifunctional oxygen electrocatalysts at low cost for rechargeable Zn-air batteries. Chem. Commun. **51**, 8841–8844 (2015)
27. Hadidi, L., Davari, E., Iqbal, M., et al.: Spherical nitrogen-doped hollow mesoporous carbon as an efficient bifunctional electrocatalyst for Zn-air batteries. Nanoscale **7**, 20547–20556 (2015)
28. Shinde, S.S., Lee, C.H., Sami, A., et al.: Scalable 3-D carbon nitride sponge as an efficient metal-free bifunctional oxygen electrocatalyst for rechargeable Zn-air batteries. ACS Nano **11**, 347–357 (2017)
29. Hu, C., Dai, L.: Multifunctional carbon-based metal-free electrocatalysts for simultaneous oxygen reduction, oxygen evolution, and hydrogen evolution. Adv. Mater. **29**, 1604942 (2017)
30. Davodi, F., Tavakkoli, M., Lahtinen, J., et al.: Straightforward synthesis of nitrogen-doped carbon nanotubes as highly active bifunctional electrocatalysts for full water splitting. J. Catal. **353**, 19–27 (2017)
31. Yue, X., Huang, S.L., Cai, J.J., et al.: Heteroatoms dual doped porous graphene nanosheets as efficient bifunctional metal-free electrocatalysts for overall water-splitting. J. Mater. Chem. A **5**, 7784–7790 (2017)
32. Roy-Mayhew, J.D., Bozym, D.J., Punckt, C., et al.: Functionalized graphene as a catalytic counter electrode in dye-sensitized solar cells. ACS Nano **4**, 6203–6211 (2010)
33. Xue, Y., Liu, J., Chen, H., Wang, R., et al.: Nitrogen-doped graphene foams as metal-free counter electrodes in high-performance dye-sensitized solar cells. Angew. Chem. Int. Ed. **51**, 12124–12127 (2012)
34. Seo, S.H., Kim, S.Y., Koo, B.K., et al.: Influence of electrolyte composition on the photovoltaic performance and stability of

dye-sensitized solar cells with multiwalled carbon nanotube catalysts. Langmuir **26**, 10341–10346 (2010)
35. Cha, S.I., Koo, B.K., Seo, S.H., et al.: Pt-free transparent counter electrodes for dye-sensitized solar cells prepared from carbon nanotube micro-balls. J. Mater. Chem. **20**, 659–662 (2010)
36. Kumar, B., Asadi, M., Pisasale, D., et al.: Renewable and metal-free carbon nanofibre catalysts for carbon dioxide reduction. Nat. Commun. **4**, 2819 (2013)
37. Sharma, P.P., Wu, J.J., Yadav, R.M., et al.: Nitrogen-doped carbon nanotube arrays for high-efficiency electrochemical reduction of CO_2: on the understanding of defects, defect density, and selectivity. Angew. Chem. Int. Ed. **54**, 13701–13705 (2015)
38. Wu, J.J., Liu, M.J., Sharma, P.P., et al.: Incorporation of nitrogen defects for efficient reduction of CO_2 via two-electron pathway on three-dimensional graphene foam. Nano Lett. **16**, 466–470 (2016)
39. Xu, J., Kan, Y., Huang, R., et al.: Revealing the origin of activity in nitrogen-doped nanocarbons towards electrocatalytic reduction of carbon dioxide. ChemSusChem **9**, 1085–1089 (2016)
40. Zhang, S., Kang, P., Ubnoske, S., et al.: Polyethylenimine-enhanced electrocatalytic reduction of CO_2 to formate at nitrogen-doped carbon nanomaterial. J. Am. Chem. Soc. **136**, 7845–7848 (2014)
41. Qie, L., Lin, Y., Connell, J., et al.: Highly rechargeable lithium-CO_2 batteries with a boron-and nitrogen-codoped holey-graphene cathode. Angew. Chem. Int. Ed. **56**, 6970–6974 (2017)
42. Hu, X., Li, Z., Chen, J.: Flexible Li-CO_2 batteries with liquid-free electrolyte. Angew. Chem. Int. Ed. **56**, 5785–5789 (2017)
43. Kroto, H.W., Heath, J.R., Obrien, S.C., et al.: C60: buckminsterfullerene. Nature **318**, 162–163 (1985)
44. Dai, L. (ed.): Carbon Nanotechnology: Recent Developments in Chemistry, Physics, Materials Science and Device Applications. Elsevier, Amsterdam (2006)
45. Zhu, Z., Wei, N., Xie, H., et al.: Acoustic-assisted assembly of an individual monochromatic ultralong carbon nanotube for high on-current transistors. Sci. Adv. **2**, e1601572 (2016)
46. Zhang, R.F., Zhang, Y.Y., Zhang, Q., et al.: Growth of half-meter long carbon nanotubes based on Schulz–Flory distribution. ACS Nano **7**, 6156–6161 (2013)
47. Dresselhaus, M.: Carbon connections promise nanoelectronics. Phys. World **9**, 18 (1996)
48. Peigney, A., Laurent, C., Flahaut, E., et al.: Specific surface area of carbon nanotubes and bundles of carbon nanotubes. Carbon **39**, 507–514 (2001)
49. Lu, X., Chen, Z.F.: Curved pi-conjugation, aromaticity, and the related chemistry of small fullerenes. Chem. Rev. **105**, 3643–3696 (2005)
50. Tasis, D., Tagmatarchis, N., Bianco, A., et al.: Chemistry of carbon nanotubes. Chem. Rev. **106**, 1105–1136 (2006)
51. Karousis, N., Tagmatarchis, N., Tasis, D.: Current progress on the chemical modification of carbon nanotubes. Chem. Rev. **110**, 5366–5397 (2010)
52. Qu, L., Du, F., Dai, L.: Preferential syntheses of semiconducting vertically aligned single-walled carbon nanotubes for direct use in FETs. Nano Lett. **8**, 2682–2687 (2008)
53. Planeix, J.M., Coustel, N., Coq, B., et al.: Application of carbon nanotubes as supports in heterogeneous catalysis. J. Am. Chem. Soc. **116**, 7935–7936 (1994)
54. Serp, P., Corrias, M., Kalck, P.: Carbon nanotubes and nanofibers in catalysis. Appl. Catal. A Gen. **253**, 337–358 (2003)
55. An, K.H., Kim, W.S., Park, Y.S., et al.: Electrochemical properties of high-power supercapacitors using single-walled carbon nanotube electrodes. Adv. Funct. Mater. **11**, 387–392 (2001)
56. Welna, D., Qu, L., Taylor, B., et al.: Vertically aligned carbon nanotube electrodes for lithium-ion batteries. J. Power Sources **196**, 1455–1460 (2011)
57. Zhang, S., Kang, L., Wang, X., et al.: Arrays of horizontal carbon nanotubes of controlled chirality grown using designed catalysts. Nature **543**, 234–238 (2017)
58. Yu, D., Nagelli, E., Du, F., et al.: Metal-free carbon nanomaterials become more active than metal catalysts and last longer. J. Phys. Chem. Lett. **1**, 2165–2173 (2010)
59. Novoselov, K.S., Geim, A.K., Morozov, S.V., et al.: Electric field effect in atomically thin carbon films. Science **306**, 666–669 (2004)
60. Geim, A.K., Novoselov, K.S.: The rise of graphene. Nat. Mater. **6**, 183–191 (2007)
61. Balandin, A.A., Ghosh, S., Bao, W.Z., et al.: Superior thermal conductivity of single-layer graphene. Nano Lett. **8**, 902–907 (2008)
62. Lee, C., Wei, X.D., Kysar, J.W., et al.: Measurement of the elastic properties and intrinsic strength of monolayer graphene. Science **321**, 385–388 (2008)
63. Novoselov, K.S.: Positive and negative oxygen vacancies in amorphous silica. ECS Trans. **19**, 3–17 (2009)
64. Qu, L., Liu, Y., Baek, J., et al.: Nitrogen-doped graphene as efficient metal-free electrocatalyst for oxygen reduction in fuel cells. ACS Nano **4**, 1321–1326 (2010)
65. Yu, D., Nagelli, E., Du, F., et al.: Carbon nanomaterials in biosensors: should you use nanotubes or graphene? Angew. Chem. Int. Ed. **49**, 2114–2138 (2010)
66. Xie, X., Qu, L., Zhou, C., et al.: An asymmetrically surface-modified graphene film electrochemical actuator. ACS Nano **4**, 6050–6054 (2010)
67. Orimo, S., Majer, G., Fukunaga, T., et al.: Hydrogen in the mechanically prepared nanostructured graphite. Appl. Phys. Lett. **75**, 3093–3095 (1999)
68. Muto, S., Kimura, T., Tanabe, T., et al.: Transmission electron microscopy and electron energy-loss spectroscopy analysis of hydrogenated nanostructured graphite prepared by mechanical milling. Jpn. J. Appl. Phys. **44**, 2061 (2005)
69. Ali, M., Urgen, M.: Simultaneous growth of diamond and nanostructured graphite thin films by hot-filament chemical vapor deposition. Solid State Sci. **14**, 150–154 (2012)
70. McCauley, T.G., Corrigan, T.D., Krauss, A.R., et al.: Electron emission properties of Si field emitter arrays coated with nanocrystalline diamond from fullerene precursors. Mater. Res. Soc. Symp. Proc. **498**, 227 (1998)
71. Xing, Y., Dai, L.: Nanodiamonds for nanomedicine. Nanomedicine (London, UK) **4**, 207 (2009)
72. Mochalin, V.N., Shenderova, O., Ho, D., et al.: The properties and applications of nanodiamonds. Nat. Nanotechnol. **7**, 11–23 (2012)
73. Liu, Y.M., Chen, S., Quan, X., et al.: Boron and nitrogen codoped nanodiamond as an efficient metal-free catalyst for oxygen reduction reaction. J. Phys. Chem. C **117**, 14992–14998 (2013)
74. Gu, W.T., Peters, N., Yushin, G.: Functionalized carbon onions, detonation nanodiamond and mesoporous carbon as cathodes in Li-ion electrochemical energy storage devices. Carbon **53**, 292–301 (2013)
75. Shenderova, O.A., Zhirnov, V.V., Brenner, D.W.: Carbon nanostructures. Crit. Rev. Solid State Mater. Sci. **27**, 227–356 (2002). **(references cited therein)**
76. Kruger, A., Kataoka, F., Ozawa, M., et al.: Unusually tight aggregation in detonation nanodiamond: identification and disintegration. Carbon **43**, 1722–1730 (2005)
77. Gruen, D.: Ultrananocrystalline diamond films from fullerene precursors. In: Osawa, E., (ed.) Perspectives of Fullerene Nanotechnology. Springer, Dortrecht (2002)
78. Krauss, A.R., Auciello, O., Gruen, D.M., et al.: Ultrananocrystalline diamond thin films for MEMS and moving mechanical assembly devices. Diam. Relat. Mater. **10**, 1952–1961 (2001)

79. Swain, G.M., Anderson, A.B., Angus, J.C.: Applications of diamond thin films in electrochemistry. MRS Bull. **23**, 56–60 (1998)
80. Chen, Z.P., Ren, W.C., Gao, L.B., et al.: Three-dimensional flexible and conductive interconnected graphene networks grown by chemical vapour deposition. Nat. Mater. **10**, 424–428 (2011)
81. Du, F., Yu, D., Dai, L., et al.: Preparation of tunable 3D pillared carbon nanotube-graphene networks for high-performance capacitance. Chem. Mater. **23**, 4810–4816 (2011)
82. Wang, D.W., Su, D.S.: Heterogeneous nanocarbon materials for oxygen reduction reaction. Energy Environ. Sci. **7**, 576–591 (2014)
83. Daems, N., Sheng, X., Vankelecom, I.F.J., et al.: Metal-free doped carbon materials as electrocatalysts for the oxygen reduction reaction. J. Mater. Chem. A **2**, 4085–4110 (2014)
84. Zheng, Y., Jiao, Y., Jaroniec, M., et al.: Nanostructured metal-free electrochemical catalysts for highly efficient oxygen reduction. Small **8**, 3550–3566 (2012)
85. Gong, K., Du, F., Xia, Z., et al.: Nitrogen-doped carbon nanotube arrays with high electrocatalytic activity for oxygen reduction. Science **323**, 760–764 (2009)
86. Zhao, Z., Li, M., Zhang, L., et al.: Design principles for heteroatom-doped carbon nanomaterials as highly efficient catalysts for fuel cells and metal-air batteries. Adv. Mater. **27**, 6834–6840 (2015)
87. Zhang, L., Xi, Z.: Mechanisms of oxygen reduction reaction on nitrogen-doped graphene for fuel cells. J. Phys. Chem. C **115**, 11170–11176 (2011)
88. Yang, L.J., Jiang, S.J., Zhao, Y., et al.: Boron-doped carbon nanotubes as metal-free electrocatalysts for the oxygen reduction reaction. Angew. Chem. Int. Ed. **50**, 7132–7135 (2011)
89. Jeon, I., Zhang, S., Zhang, L., et al.: Edge-selectively sulfurized graphene nanoplatelets as efficient metal-free electrocatalysts for oxygen reduction reaction: the electron spin effect. Adv. Mater. **25**, 6138–6145 (2013)
90. Ding, W., Wei, Z.D., Chen, S.G., et al.: Space-confinement-induced synthesis of pyridinic-and pyrrolic-nitrogen-doped graphene for the catalysis of oxygen reduction. Angew. Chem. Int. Ed. **52**, 11755–11759 (2013)
91. Guo, D.H., Shibuya, R., Akiba, C., et al.: Active sites of nitrogen-doped carbon materials for oxygen reduction reaction clarified using model catalysts. Science **351**, 361–365 (2016)
92. Zhang, H.R., Liang, E.J., Ding, P., et al.: Production and growth mechanisms of BCN nanotubes. Acta Phys. Sin. **51**, 2901–2905 (2002)
93. Yang, H., Miao, J., Hung, S., et al.: Identification of catalytic sites for oxygen reduction and oxygen evolution in N-doped graphene materials: development of highly efficient metal-free bifunctional electrocatalyst. Sci. Adv. **2**, e1501122 (2016)
94. Xiang, Z., Dai, Q., Chen, J., et al.: Edge functionalization of graphene and two-dimensional covalent organic polymers for energy conversion and storage. Adv. Mater. **28**, 6253–6261 (2016). **and references cited therein**
95. Wang, B., Hu, C., Dai, L.: Functionalized carbon nanotubes and graphene-based materials for energy storage. Chem. Commun. **52**, 14350–14360 (2016)
96. Shen, A., Zou, Y., Wang, Q., et al.: Oxygen reduction reaction in a droplet on graphite: direct evidence that the edge is more active than the basal plane. Angew. Chem. Int. Ed. **53**, 10804–10808 (2014)
97. Jeon, I., Choi, H., Choi, M., et al.: Facile, scalable synthesis of edge-halogenated graphene nanoplatelets as efficient metal-free electrocatalysts for oxygen reduction reaction. Sci. Rep. **3**, 1810 (2013)
98. Jeon, I., Choi, H., Jung, S., et al.: Large-scale production of edge-selectively functionalized graphene nanoplatelets via ball milling and their use as metal-free electrocatalysts for oxygen reduction reaction. J. Am. Chem. Soc. **135**, 1386–1393 (2013)
99. Jeon, I., Bae, S., Seo, J., et al.: Scalable production of edge-functionalized graphene nanoplatelets via mechanochemical ball-milling. Adv. Funct. Mater. **25**, 6961–6975 (2015)
100. Fan, X., Chang, D., Chen, X., et al.: Functionalized graphene nanoplatelets from ball milling for energy applications. Curr. Opin. Chem. Eng. **11**, 52–58 (2016)
101. Jeon, I., Choi, M., Choi, H., et al.: Antimony-doped graphene nanoplatelets. Nature Commun. **6**, 7123 (2015)
102. Ju, M., Jeon, I., Kim, H., et al.: Edge-selenated graphene nanoplatelets as durable metal-free catalysts for iodine reduction reaction in dye-sensitized solar cells. Sci. Adv. **56**, e1501459 (2016)
103. Kim, H., Jeon, I., Choi, I., et al.: Edge-selectively antimony-doped graphene nanoplatelets as an outstanding counter electrode with an unusual electrochemical stability for dye-sensitized solar cells employing cobalt electrolytes. J. Mater. Chem. A **4**, 9029–9037 (2016)
104. Zhang, J., Qu, L., Shi, G., et al.: N, P-codoped carbon networks as efficient metal-free bifunctional catalysts for oxygen reduction and hydrogen evolution reactions. Angew. Chem. Int. Ed. **55**, 2270–2274 (2016)
105. Qu, K.G., Zheng, Y., Zhang, X.X., et al.: Promotion of electrocatalytic hydrogen evolution reaction on nitrogen-doped carbon nanosheets with secondary heteroatom. ACS Nano **11**, 7293–7300 (2017)
106. Zhang, W., Lin, C.T., Liu, K.K., et al.: Opening an electrical band gap of bilayer graphene with molecular doping. ACS Nano **5**, 7517–7524 (2011)
107. Wang, S., Yu, D., Dai, L.: Polyelectrolyte functionalized carbon nanotubes as efficient metal-free electrocatalysts for oxygen reduction. J. Am. Chem. Soc. **133**, 5182–5185 (2011)
108. Wang, S., Yu, D., Dai, L., et al.: Polyelectrolyte-functionalized graphene as metal-free electrocatalysts for oxygen reduction. ACS Nano **5**, 6202–6209 (2011)
109. Jiao, M.G., Song, W., Li, K., et al.: First-principles study on nitrobenzene-doped graphene as a metal-free electrocatalyst for oxygen reduction reaction. J. Phys. Chem. C **120**, 8804–8812 (2016)
110. Tang, C., Zhang, Q.: Nanocarbon for oxygen reduction electrocatalysis: dopants, edges, and defects. Adv. Mater. **29**, 1604103–1604111 (2017)
111. Tang, C., Wang, H.F., Chen, X., et al.: Topological defects in metal-free nanocarbon for oxygen electrocatalysis. Adv. Mater. **28**, 6845–6851 (2016)
112. Yan, D., Li, Y., Huo, J., et al.: Defect chemistry of non-precious metal electrocatalysts for oxygen reactions. Adv. Mater. **29**, 1606459 (2017)
113. Castro Neto, A.H., Guinea, F., Peres, N.M.R., et al.: The electronic properties of graphene. Rev. Mod. Phys. **81**, 109–162 (2009)
114. Banhart, F., Kotakoski, J., Krasheninnikov, A.V.: Structural defects in graphene. ACS Nano **5**, 26–41 (2011)
115. Liu, Z., Zhao, Z., Wang, Y., et al.: In situ exfoliated, edge-rich, oxygen-functionalized graphene from carbon fibers for oxygen electrocatalysis. Adv. Mater. **29**, 1606207 (2017)
116. Chai, G.L., Hou, Z.F., Shu, D.J., et al.: Active sites and mechanisms for oxygen reduction reaction on nitrogen-doped carbon alloy catalysts: Stone–Wales defect and curvature effect. J. Am. Chem. Soc. **136**, 13629–13640 (2014)
117. Zhang, L., Niu, J., Dai, L., et al.: Effect of microstructure of nitrogen-doped graphene on oxygen reduction activity in fuel cells. Langmuir **28**, 7542–7550 (2012)
118. Zhang, L., Xu, Q., Niu, J., et al.: Role of lattice defects in catalytic activities of graphene clusters for fuel cells. Phys. Chem. Chem. Phys. **17**, 16733–16743 (2015)

119. Jin, H., Huang, H., He, Y., et al.: Graphene quantum dots supported by graphene nanoribbons with ultrahigh electrocatalytic performance for oxygen reduction. J. Am. Chem. Soc. **137**, 7588–7591 (2015)
120. Jiang, Y., Yang, L., Sun, T., et al.: Significant contribution of intrinsic carbon defects to oxygen reduction activity. ACS Catal. **5**, 6707–6712 (2015)
121. Jia, Y., Zhang, L., Du, A., et al.: Defect graphene as a trifunctional catalyst for electrochemical reactions. Adv. Mater. **28**, 9532–9538 (2016)
122. Zhao, X., Zou, X., Yan, X., et al.: Defect-driven oxygen reduction reaction (ORR) of carbon without any element doping. Inorg. Chem. Front. **3**, 417–421 (2016)
123. Su, D.S., Perathoner, S., Centi, G.: Nanocarbons for the development of advanced catalysts. Chem. Rev. **113**, 5782–5816 (2013)
124. Sharma, R., Baik, J.H., Perera, C.J., et al.: Anomalously large reactivity of single graphene layers and edges toward electron transfer chemistries. Nano Lett. **10**, 398–405 (2010)
125. Yuan, W., Zhou, Y., Li, Y., et al.: The edge-and basal-plane-specific electrochemistry of a single-layer graphene sheet. Sci. Rep. **3**, 2248 (2013)
126. Tao, L., Wang, Q., Dou, S., et al.: Edge-rich and dopant-free graphene as a highly efficient metal-free electrocatalyst for the oxygen reduction reaction. Chem. Commun. **52**, 2764–2767 (2016)
127. Wang, S., Iyyamperumal, E., Roy, A., et al.: Vertically aligned BCN nanotubes as efficient metal-free electrocatalysts for the oxygen reduction reaction: a synergetic effect by co-doping with boron and nitrogen. Angew. Chem. Int. Ed. **50**, 11756–11760 (2011)
128. Zhao, Y., Yang, L., Chen, S., et al.: Can boron and nitrogen co-doping improve oxygen reduction reaction activity of carbon nanotubes? J. Am. Chem. Soc. **135**, 1201–1204 (2013)
129. Zheng, Y., Jiao, Y., Ge, L., et al.: Two-step boron and nitrogen doping in graphene for enhanced synergistic catalysis. Angew. Chem. **125**, 3192–3198 (2013)
130. Tian, G.L., Zhang, Q., Zhang, B.S., et al.: Toward full exposure of "active sites": nanocarbon electrocatalyst with surface enriched nitrogen for superior oxygen reduction and evolution reactivity. Adv. Funct. Mater. **24**, 5956–5961 (2014)
131. Qu, K.G., Zheng, Y., Jiao, Y., et al.: Polydopamine-inspired, dual heteroatom-doped carbon nanotubes for highly efficient overall water splitting. Adv. Energy Mater. **7**, 1602068 (2017)
132. Zheng, Y., Jiao, Y., Zhu, Y.H., et al.: Hydrogen evolution by a metal-free electrocatalyst. Nat. Commun. **5**, 3783 (2014)
133. Shinde, S.S., Sami, A., Lee, J.H.: Electrocatalytic hydrogen evolution using graphitic carbon nitride coupled with nanoporous graphene co-doped by S and Se. J. Mater. Chem. A **3**, 12810–12819 (2015)
134. Xie, G.C., Zhang, K., Guo, B.D., et al.: Graphene-based materials for hydrogen generation from light-driven water splitting. Adv. Mater. **25**, 3820–3839 (2013)
135. Katsounaros, I., Cherevko, S., Zeradjanin, A.R., et al.: Oxygen electrochemistry as a cornerstone for sustainable energy conversion. Angew. Chem. Int. Ed. **53**, 102–121 (2014)
136. Huang, X.D., Zhao, Y.F., Ao, Z.M., et al.: Micelle-template synthesis of nitrogen-doped mesoporous graphene as an efficient metal-free electrocatalyst for hydrogen production. Sci. Rep. **4**, 7557 (2014)
137. Ge, J.M., Zhang, B., LV, L.B., et al.: Constructing holey graphene monoliths via supramolecular assembly: enriching nitrogen heteroatoms up to the theoretical limit for hydrogen evolution reaction. Nano Energy **15**, 567–575 (2015)
138. Chen, S., Duan, J.J., Jaroniec, M., et al.: Nitrogen and oxygen dual-doped carbon hydrogel film as a substrate-free electrode for highly efficient oxygen evolution reaction. Adv. Mater. **26**, 2925–2930 (2014)
139. Othman, R., Dicks, A.L., Zhu, Z.H.: Non precious metal catalysts for the PEM fuel cell cathode. Int. J. Hydrogen Energy **37**, 357–372 (2012)
140. Hamilton, P.J., Pollet, B.G.: Polymer electrolyte membrane fuel cell (PEMFC) flow field plate: design, materials and characterisation. Fuel Cells **10**, 489–509 (2010)
141. Wang, S.Y., Jiang, S.P.: Prospects of fuel cell technologies. Natl. Sci. Rev. **4**, 163–166 (2017)
142. Appleby, A.J.: Electrocatalysis of aqueous dioxygen reduction. J. Electroanal. Chem. **357**, 117–179 (1993)
143. Schmidt, T.J., Markovic, N.M.: Encyclopedia of Surface and Colloid Science. Taylor & Francis, New York (2006)
144. Rao, C.V., Ishikawa, Y.: Activity, selectivity, and anion-exchange membrane fuel cell performance of virtually metal-free nitrogen-doped carbon nanotube electrodes for oxygen reduction reaction. J. Phys. Chem. C **116**, 4340–4346 (2012)
145. Yu, D., Zhang, Q., Dai, L.: Highly efficient metal-free growth of nitrogen-doped single-walled carbon nanotubes on plasma-etched substrates for oxygen reduction. J. Am. Chem. Soc. **132**, 15127–15129 (2010)
146. Xiang, Z., Xue, Y., Cao, D., et al.: Highly efficient electrocatalysts for oxygen reduction based on 2D covalent organic polymers complexed with non-precious metals. Angew. Chem. Int. Ed. **53**, 2433–2437 (2014)
147. Kundu, S., Nagaiah, T.C., Xia, W., et al.: Electrocatalytic activity and stability of nitrogen-containing carbon nanotubes in the oxygen reduction reaction. J. Phys. Chem. C **113**, 14302–14310 (2009)
148. Wang, X.Q., Lee, J.S., Zhu, Q., et al.: Ammonia-treated ordered mesoporous carbons as catalytic materials for oxygen reduction reaction. Chem. Mater. **22**, 2178–2180 (2010)
149. Li, Y.G., Zhou, W., Wang, H.L., et al.: An oxygen reduction electrocatalyst based on carbon nanotube-graphene complexes. Nat. Nanotechnol. **7**, 394–400 (2012)
150. Shi, Q.Q., Peng, F., Liao, S.X., et al.: Sulfur and nitrogen co-doped carbon nanotubes for enhancing electrochemical oxygen reduction activity in acidic and alkaline media. J. Mater. Chem. A **1**, 14853–14857 (2013)
151. Xiong, W., Du, F., Liu, Y., et al.: 3-D carbon nanotube structures used as high performance catalyst for oxygen reduction reaction. J. Am. Chem. Soc. **132**, 15839–15841 (2010)
152. Winther-Jensen, B., Winther-Jensen, O., Forsyth, M., et al.: High rates of oxygen reduction over a vapor phase–polymerized PEDOT electrode. Science **321**, 671–674 (2008)
153. Choi, C.H., Chung, M.W., Kwon, H.C., et al.: Nitrogen-doped graphene/carbon nanotube self-assembly for efficient oxygen reduction reaction in acid media. Appl. Catal. B Environ. **144**, 760–766 (2014)
154. Gouse, P.S., Sahu, A.K., Arunchander, A., et al.: Nitrogen and fluorine co-doped graphite nanofibers as high durable oxygen reduction catalyst in acidic media for polymer electrolyte fuel cells. Carbon **93**, 130–142 (2015)
155. Zhang, J., Dai, L.: Nitrogen, phosphorus, and fluorine tri-doped graphene as a multifunctional catalyst for self-powered electrochemical water splitting. Angew. Chem. Int. Ed. **55**, 13296–13300 (2016)
156. Pei, Z.X., Gu, J.X., Wang, Y.K., et al.: Component matters: paving the roadmap toward enhanced electrocatalytic performance of graphitic C3N4-based catalysts via atomic tuning. ACS Nano **11**, 6004–6014 (2017)
157. Li, X.H., Antonietti, M.: Polycondensation of boron-and nitrogen-codoped holey graphene monoliths from molecules: carbocatalysts for selective oxidation. Angew. Chem. Int. Ed. **52**, 457–4576 (2013)

158. Lai, J.P., Li, S.P., Wu, F.X., et al.: Unprecedented metal-free 3D porous carbonaceous electrodes for full water splitting. Energy Environ. Sci. **9**, 1210–1214 (2016)
159. Meng, Y.Y., Voiry, D., Goswami, A., et al.: N-, O-, and S-tri-doped nanoporous carbons as selective catalysts for oxygen reduction and alcohol oxidation reactions. J. Am. Chem. Soc. **136**, 13554–13557 (2014)
160. Li, F.J., Zhang, T., Zhou, H.S.: Challenges of non-aqueous Li-O_2 batteries: electrolytes, catalysts, and anodes. Energy Environ. Sci. **6**, 1125–1141 (2013)
161. Imanishi, N., Yamamoto, O.O.: Rechargeable lithium-air batteries: characteristics and prospects. Mater. Today **17**, 24–30 (2014)
162. Dou, S., Li, X.Y., Tao, L., et al.: Cobalt nanoparticle-embedded carbon nanotube/porous carbon hybrid derived from MOF-encapsulated Co_3O_4 for oxygen electrocatalysis. Chem. Commun. **52**, 9727–9730 (2016)
163. Kwak, W.J., Jung, H.G., Aurbach, D., et al.: Optimized bicompartment two solution cells for effective and stable operation of Li-O_2 batteries. Adv. Energy Mater. **7**, 1701232 (2017)
164. Hu, C., Wang, L., Zhao, Y., et al.: Designing nitrogen-enriched echinus-like carbon capsules for highly efficient oxygen reduction reaction and lithium ion storage. Nanoscale **6**, 8002–8009 (2014)
165. Meng, W., Wen, L.N., Song, Z.H., et al.: Metal-free boron-doped carbon microspheres as excellent cathode catalyst for rechargeable Li-O_2 battery. J. Solid State Electrochem. **21**, 665–671 (2017)
166. Shu, C.Z., Lin, Y.M., Su, D.S.: N-doped onion-like carbon as an efficient oxygen electrode for long-life Li-O_2 battery. J. Mater. Chem. A **4**, 2128–2136 (2016)
167. Shui, J., Du, F., Xue, C., et al.: Vertically aligned N-doped coral-like carbon fiber arrays as efficient air electrodes for high-performance nonaqueous Li-O_2 batteries. ACS Nano **8**, 3015–3022 (2014)
168. Lim, K.H., Kweon, H.J., Kim, H.S.: Polydopamine-derived nitrogen-doped graphitic carbon for a bifunctional oxygen electrode in a non-aqueous Li-O_2 battery. J. Electrochem. Soc. **164**, A1595–A1600 (2017)
169. Kang, J.W., Kim, D.Y., Suk, J.D., et al.: Enhanced energy and O_2 evolution efficiency using an in situ electrochemically N-doped carbon electrode in non-aqueous Li-O_2 batteries. J. Mater. Chem. A **3**, 18843–18846 (2015)
170. Xing, Z.Y., Luo, X.Y., Qi, Y.T., et al.: Nitrogen-doped nanoporous graphenic carbon: an efficient conducting support for O_2 cathode. ChemNanoMat **2**, 692–697 (2016)
171. Lin, H., Liu, Z.X., Mao, Y.X., et al.: Effect of nitrogen-doped carbon/Ketjen black composite on the Morphology of Li_2O_2 for high-energy-density Li-air batteries. Carbon **96**, 965–971 (2016)
172. Elia, G.A., Hassoun, J., Kwak, W.J., et al.: An advanced lithium-air battery exploiting an ionic liquid-based electrolyte. Nano Lett. **14**, 6572–6577 (2014)
173. Mi, R., Liu, H., Wang, H., et al.: Effects of nitrogen-doped carbon nanotubes on the discharge performance of Li-air batteries. Carbon **67**, 744–752 (2014)
174. Li, J., Peng, B., Zhou, G., et al.: Partially cracked carbon nanotubes as cathode materials for lithium-air batteries. ECS Electrochem. Lett. **2**, A25–A27 (2013)
175. Cao, R.G., Lee, J.S., Liu, M.L., et al.: Recent progress in non-precious catalysts for metal-air batteries. Adv. Energy Mater. **2**, 816–829 (2012)
176. Lakes, R.: Materials with structural hierarchy. Nature **361**, 511 (1993)
177. Zhou, W., Zhang, H.Z., Nie, H.J., et al.: Hierarchical micron-sized mesoporous/macroporous graphene with well-tuned surface oxygen chemistry for high capacity and cycling stability Li-O_2 battery. ACS Appl. Mater. Interfaces **7**, 3389–3397 (2015)
178. Ding, N.S., Chien, W., Hor, A.: Influence of carbon pore size on the discharge capacity of Li-O_2 Batteries. J. Mater. Chem. **2**, 12433–12441 (2014)
179. Liu, S., Wang, Z., Yu, C., et al.: Free-standing, hierarchically porous carbon nanotube film as a binder-free electrode for high-energy Li-O_2 batteries. J. Mater. Chem. A **1**, 12033–12037 (2013)
180. Li, Y.G., Dai, H.J.: Recent advances in zinc-air batteries. Chem. Soc. Rev. **43**, 5257–5275 (2014)
181. Xu, M., Ivey, D.G., Xie, Z., et al.: Rechargeable Zn-air batteries: progress in electrolyte development and cell configuration advancement. J. Power Sources **283**, 358–371 (2015)
182. Lee, J.S., Kim, S.T., Cao, R., et al.: Metal-air batteries with high energy density: Li-air versus Zn-air. Adv. Energy Mater. **1**, 34–50 (2011)
183. Chen, S., Duan, J.J., Zheng, Y., et al.: Ionic liquid-assisted synthesis of N/S-double doped graphene microwires for oxygen evolution and Zn-air batteries. Energy Storage Mater. **1**, 17–24 (2015)
184. Liu, Q., Wang, Y., Dai, L., et al.: Scalable fabrication of nanoporous carbon fiber films as bifunctional catalytic electrodes for flexible Zn-air batteries. Adv. Mater. **28**, 3000–3006 (2016)
185. Zhao, Y., Nakamura, R., Kamiya, K., et al.: Nitrogen-doped carbon nanomaterials as non-metal electrocatalysts for water oxidation. Nat. Commun. **4**, 2390 (2013)
186. Yu, X.W., Zhang, M., Chen, J., et al.: Nitrogen and sulfur codoped graphite foam as a self-supported metal-free electrocatalytic electrode for water oxidation. Adv. Energy Mater. **6**, 1501492 (2016)
187. Lei, Y.J., Wei, L., Zhai, S.L., et al.: Metal-free bifunctional carbon electrocatalysts derived from zeolitic imidazolate frameworks for efficient water splitting. Mater. Chem. Front. **2**, 102–111 (2018)
188. Zhang, Z.Y., Yi, Z.R., Wang, J., et al.: Nitrogen-enriched polydopamine analogue-derived defect-rich porous carbon as a bifunctional metal-free electrocatalyst for highly efficient overall water splitting. J. Mater. Chem. A **5**, 17064–17072 (2017)
189. Hu, C., Chen, X., Dai, Q.: Earth-abundant carbon catalysts for renewable generation of clean energy from sunlight and water. Nano Energy **41**, 367–376 (2017)
190. Wang, S., Zhang, L., Xia, Z., et al.: BCN graphene as efficient metal-free electrocatalyst for the oxygen reduction reaction. Angew. Chem. Int. Ed. **51**, 4209–4212 (2012)
191. Liu, J., Liu, Y., Liu, N., et al.: Metal-free efficient photocatalyst for stable visible water splitting via a two-electron pathway. Science **347**, 970–974 (2015)
192. Wu, M.X., Lin, X., Wang, T.H., et al.: Low-cost dye-sensitized solar cell based on nine kinds of carbon counter electrodes. Energy Environ. Sci. **4**, 2308–2315 (2011)
193. Brennan, L.J., Byrne, M.T., Bari, M., et al.: Carbon nanomaterials for dye-sensitized solar cell applications: a bright future. Adv. Energy Mater. **1**, 472–485 (2011)
194. Lee, K.S., Lee, W.J., Park, N.G., et al.: Transferred vertically aligned N-doped carbon nanotube arrays: use in dye-sensitized solar cells as counter electrode. Chem. Commun. **47**, 4264–4266 (2011)
195. Dong, P., Pint, C.L., Hainey, M., et al.: Vertically aligned single-walled carbon nanotubes as low-cost and high electrocatalytic counter electrode for dye-sensitized solar cells. ACS Appl. Mater. Interfaces **3**, 3157–3161 (2011)
196. Li, S., Luo, Y., Lv, W., et al.: Vertically aligned carbon nanotubes grown on graphene paper as electrodes in lithium-ion batteries and dye-sensitized solar cells. Adv. Energy Mater. **1**, 486–490 (2011)
197. Lu, K., Hu, Z., Ma, J., et al.: A rechargeable iodine-carbon battery that exploits ion intercalation and iodine redox chemistry. Nat. Commun. **8**, 527 (2017)
198. Wang, Y.L., Sun, Q.L., Zhao, Q.Q., et al.: Rechargeable lithium/iodine battery with superior high-rate capability by using

iodine-carbon composite as cathode. Energy Environ. Sci. **4**, 3947–3950 (2011)
199. Zhao, Q., Lu, Y., Zhu, Z., et al.: Rechargeable lithium-iodine batteries with iodine/nanoporous carbon cathode. Nano Lett. **15**, 5982–5987 (2015)
200. Zhao, Y., Hong, M., Mercier, N.B., et al.: A 3.5 V lithium-iodine hybrid redox battery with vertically aligned carbon nanotube current collector. Nano Lett. **14**, 1085–1092 (2014)
201. Su, Z., Tong, C.J., He, D.Q., et al.: Ultra-small B_2O_3 nanocrystals grown in situ on highly porous carbon microtubes for lithium-iodine and lithium-sulfur batteries. J. Mater. Chem. A **4**, 8541–8547 (2016)
202. Zhang, C., Mahmood, N., Yin, H., et al.: Synthesis of phosphorus doped graphene and its multifunctional applications for oxygen reduction reaction and lithium ion batteries. Adv. Mater. **25**, 4932–4937 (2013)
203. Xu, J., Wang, M., Wickramaratne, N., et al.: High-performance sodium ion batteries based on a 3D anode from nitrogen-doped graphene foams. Adv. Mater. **27**, 2042–2048 (2015)
204. Duan, X.C., Xu, J.T., Wei, Z.X., et al.: Metal-free carbon materials for CO_2 electrochemical reduction. Adv. Mater. **29**, 1701784 (2017)
205. Kuhl, K.P., Hatsukade, T., Cave, E.R., et al.: Electrocatalytic conversion of carbon dioxide to methane and methanol on transition metal surfaces. J. Am. Chem. Soc. **136**, 14107–14113 (2014)
206. Wu, J.J., Yadav, R.M., Liu, M.J., et al.: Achieving highly efficient, selective, and stable CO_2 reduction on nitrogen-doped carbon nanotubes. ACS Nano **9**, 5364–5371 (2015)
207. Sreekanth, N., Nazrulla, M.A., Vineesh, T.V., et al.: Metal-free boron-doped graphene for selective electroreduction of carbon dioxide to formic acid/formate. Chem. Commun. **51**, 1606–16064 (2015)
208. Nakata, K., Ozaki, T., Terashima, C., et al.: High-yield electrochemical production of formaldehyde from CO_2 and seawater. Angew. Chem. Int. Ed. **53**, 871–874 (2014)
209. Liu, Y., Chen, S., Quan, X., et al.: Efficient electrochemical reduction of carbon dioxide to acetate on nitrogen-doped nanodiamond. J. Am. Chem. Soc. **137**, 11631–11636 (2015)
210. Lu, X., Tan, T.H., Ng, Y.H., et al.: Highly selective and stable reduction of CO_2 to CO by a graphitic carbon nitride/carbon nanotube composite electrocatalyst. Chem. Eur. J. **22**, 11991–11996 (2016)
211. Wu, J.J., Ma, S.C., Sun, J., et al.: A metal-free electrocatalyst for carbon dioxide reduction to multi-carbon hydrocarbons and oxygenate. Nat. Commun. **7**, 13869 (2016)
212. Song, Y.F., Chen, W., Zhao, C.C., et al.: Metal-free nitrogen-doped mesoporous carbon for electroreduction of CO_2 to ethanol. Angew. Chem. Int. Ed. **56**, 10840–10844 (2017)
213. Li, W., Seredych, M., Rodriguez-Castellon, E., et al.: Metal-free nanoporous carbon as a catalyst for electrochemical reduction of CO_2 to CO and CH_4. ChemSusChem **9**, 606–616 (2016)
214. Liu, Y.M., Zhang, Y.J., Cheng, K., et al.: Selective electrochemical reduction of carbon dioxide to ethanol on a boron- and nitrogen-co-doped nanodiamond. Angew. Chem. Int. Ed. **56**, 15607–15611 (2017)
215. Wang, H., Chen, Y., Hou, X., et al.: Nitrogen-doped graphenes as efficient electrocatalysts for the selective reduction of carbon dioxide to formate in aqueous solution. Green Chem. **18**, 3250–3252 (2016)
216. Sun, X., Kang, X., Zhu, Q., et al.: Very highly efficient reduction of CO_2 to CH_4 using metal-free N-doped carbon electrodes. Chem. Sci. **7**, 2883–2887 (2016)
217. Liu, Y., Chen, S., Quan, X., et al.: Tuning the electrochemical properties of a boron and nitrogen codoped nanodiamond rod array to achieve high performance for both electro-oxidation and electro-reduction. J. Mater. Chem. A **1**, 14706–14712 (2013)
218. Yokoya, T., Nakamura, T., Matsushita, T., et al.: Origin of the metallic properties of heavily boron-doped superconducting diamond. Nature **438**, 647–650 (2005)
219. Wang, H., Jia, J., Song, P., et al.: Efficient electrocatalytic reduction of CO_2 by nitrogen-doped nanoporous carbon/carbon nanotube membranes-A step towards the electrochemical CO_2 refinery. Angew. Chem. Int. Ed. **56**, 7847–7852 (2017)
220. Li, L., Manthiram, A.: O-and N-doped carbon nanowebs as metal-free catalysts for hybrid Li-air batteries. Adv. Energy Mater. **4**, 1301795 (2014)
221. Centi, G., Perathoner, S.: Opportunities and prospects in the chemical recycling of carbon dioxide to fuels. Catal. Today **148**, 191–205 (2009)

Chuangang Hu received his MS from Henan Normal University in 2011, and his Ph.D. from Beijing Institute of Technology in 2015. He is currently a postdoctoral research associate in Professor Liming Dai's group at Case Western Reserve University. His research interests focus on carbon-based materials for energy conversion and storage.

Ying Xiao received her PhD degree from Beijing Insinuate of Technology in 2015. From December of 2015 to December of 2016, she was a postdoctoral researcher at Hanyang University. She is currently a postdoctoral researcher at BUCT-CWRU International Joint Lab. Her current research interests focus on the design and synthesis of carbon-based materials and their applications in metal-air batteries.

Yuqin Zou received her bachelor and master's degree in 2012 from Shanghai University and her PhD. in 2017 from The University of Manchester. She is currently a lecturer of the College of Energy, Beijing University of Chemical Technology. Her research interests are in novel 2D materials, such as graphene, layered double hydroxide and black phosphorus, and their application in energy storages devices and electrocatalysis.

Liming Dai joined Case Western Reserve University (CWRU) in fall 2009 as the Kent Hale Smith Professor in the Department of Macromolecular Science and Engineering. He is also director of the Center of Advanced Science and Engineering for Carbon (CASE4Carbon). Dr. Dai received a B.Sc. degree from Zhejiang University in 1983, and a Ph.D. from the Australian National University in 1991. He accepted a postdoctoral fellowship from the Cavendish Laboratory at the University of Cambridge and two years later became a visiting follow at the University of Illinois at Urbana-Champaign. Dr. Dai's expertise lies across the synthesis, chemical modification and device fabrication of conjugated polymers and carbon nanomaterials for energy-related and biomedical applications.

Affiliations

Chuangang Hu[1] · Ying Xiao[1,2] · Yuqin Zou[2] · Liming Dai[1,2,3]

✉ Liming Dai
liming.dai@case.edu

[1] Center of Advanced Science and Engineering for Carbon (Case4Carbon), Department of Macromolecular Science and Engineering, Case Western Reserve University (CWRU), Cleveland, OH 44106, USA

[2] BUCT-CWRU International Joint Laboratories, College of Energy, Beijing University of Chemical Technology (BUCT), Beijing 100029, China

[3] UNSW-CWRU International Joint Laboratories, School of Chemical Engineering, University of New South Wales (UNSW), Sydney, NSW 2025, Australia